JOURNAL OF PHYSICAL ORGANIC CHEMISTRY
J. Phys. Org. Chem. 2004; **17:** 913–933
Published online in Wiley InterScience (www.interscience.wiley.com). DOI: 10.1002/poc.841

Review Commentary

A priori calculation of molecular properties to chemical accuracy†

Trygve Helgaker,[1]* Torgeir A. Ruden,[1] Poul Jørgensen,[2] Jeppe Olsen[2] and Wim Klopper[3]

[1]Department of Chemistry, University of Oslo, Box 1033 Blindern, N-0315 Oslo, Norway
[2]Department of Chemistry, Aarhus University, DK-8000 Århus C, Denmark
[3]Institute of Physical Chemistry, University of Karlsruhe (TH), D-76128 Karlsruhe, Germany

Received 28 April 2004; revised 3 June 2004; accepted 7 June 2004

ABSTRACT: Quantum chemical methods for the calculation of molecular properties to chemical accuracy are reviewed. We begin by reviewing wave-function based electronic structure theory, with emphasis on coupled-cluster theory and the description of electron correlation in terms of virtual excitations from occupied to virtual molecular orbitals. Next, we discuss the expansion of molecular orbitals in atomic orbitals and the design of one-electron basis sets for correlated calculations at the coupled-cluster level of theory. In particular, we discuss the convergence of the electronic energy in the principal expansion as realized in the correlation-consistent basis sets. Following this theoretical introduction, we consider the accurate calculation of atomization energies, reaction enthalpies, dipole moments and spectroscopic constants such as bond distances and harmonic and anharmonic force constants. For each property, we identify what levels of theory in terms of basis set (the one-electron description) and virtual excitation level (the *N*-electron description) are needed for agreement with experiment to chemical accuracy, that is, about 1 kcal mol^{-1} (1 kcal = 4.184 kJ) for atomization energies and reaction enthalpies, about 0.1 pm for bond distances and about 1 cm^{-1} for vibrational frequencies. In each case, we consider in detail the direction and magnitude of the changes in the calculated properties with improvements in the one- and *N*-electron descriptions of the electronic system, paying particular attention to the cancellation of errors arising from the simultaneous truncations of the coupled-cluster expansion and the one-electron basis set. We emphasize that agreement with experiment, even with chemical accuracy, for a few selected properties is by itself no guarantee of quality and should never be taken as indicative of an accurate description of the electronic system. To ensure such a description, the errors arising from the truncations of the one- and *N*-electron expansions must be controlled by carrying out sequences of calculations, where the different levels of theory are systematically varied and where convergence is carefully monitored. Copyright © 2004 John Wiley & Sons, Ltd.

KEYWORDS: quantum chemistry; accurate calculations; electron correlation; coupled-cluster theory; basis-set convergence; molecular properties

INTRODUCTION

The field of molecular electronic-structure theory has developed rapidly during the last few decades, allowing chemists to study theoretically systems of increasing size and complexity, often with an accuracy that rivals or even surpasses that of experimental measurements.[1–4] This situation has come about partly as a result of new developments in computational techniques and partly as a result of spectacular advances in computer technology. Consequently, the practicing chemist now has at his or her disposal a wide range of powerful techniques of varying cost and accuracy, all of which can be applied to solve problems at the microscopic and molecular levels.

In this paper, we discuss those particular methods of quantum chemistry that are capable of very high accuracy. Our purpose is not only to demonstrate what accuracy these methods are capable of in the hands of an experienced quantum chemist, but also to provide guidelines for the practicing chemist on how to carry out accurate calculations and, in particular, to show what pitfalls should be avoided when applying quantum- chemical methods in situations where high accuracy is mandatory.

**Correspondence to:* T. Helgaker, Department of Chemistry, University of Oslo, Box 1033 Blindern, N-0315, Oslo, Norway.
E-mail: trygve.helgaker@kjemi.uio.no

†Paper presented at the 9th European Symposium on Organic Reactivity, 12–17 July 2003, Oslo, Norway.

Contract/grant sponsor: Norwegian Research Council through a Strategic University Program in Quantum Chemistry; *Contract/grant number:* 154011/420.
Contract/grant sponsor: Supercomputing Programme.
Contract/grant sponsor: Danish Natural Research Council; *Contract/grant number:* 21-02-0467.
Contract/grant sponsor: Danish Center for Scientific Computing.
Contract/grant sponsor: Deutsche Forschungsgemeinschaft through the Center for Functional Nanostructures; *Contract/grant number:* CFN, Project No. C2.3.

Copyright © 2004 John Wiley & Sons, Ltd.

It should be noted immediately that not all methods of quantum chemistry are appropriate in situations where high accuracy is essential. In particular, the popular and versatile methods of density-functional theory (DFT)[5] cannot be applied when a strict control of accuracy is necessary. In such situations, we must instead turn to the hierarchical methods of quantum chemistry, in particular, to the coupled-cluster hierarchy of wave functions.[4,6–10] In this hierarchy of computational methods, it is possible to approach, in a systematic manner, the 'exact' solution to a given chemical problem, in a manner we shall discuss more precisely later.[6]

As a caveat, we note that not all problems of molecular systems and their reactions and interactions can be treated in a simple manner by coupled-cluster theory. There are problems, in particular, related to chemical reactions and to the breaking and making of chemical bonds, that are not easily treated by standard coupled-cluster theory.[11] Nevertheless, most of the chemistry related to stable molecular systems can be treated to a very high accuracy by these methods.[1] In the present review, we restrict ourselves to such systems. More specifically, we shall concentrate our attention on small (mostly organic) systems and to systems containing light atoms, where the effects of relativity are small. Coupled-cluster theory is in principle not restricted to small systems and important recent developments have extended its application range dramatically, to include molecules containing a large number of atoms.[12–18] At present, however, highly accurate applications of coupled-cluster theory are restricted to systems containing no more than 10 to 20 atoms.

THEORY

Molecular many-body problem

A stationary state of a molecular electronic system is described by an electronic wave function, a mathematical function that depends on the spatial and spin coordinates of each electron in the system [Eqn (1)]:

$$\Psi = \Psi(x_1, y_1, z_1, s_1, x_2, y_2, z_2, s_2, \ldots, x_N, y_N, z_N, s_N) \tag{1}$$

The wave function corresponds to the solution of the time-independent Schrödinger equation [Eqn (2)]:[19]

$$\hat{H}\Psi = E\Psi \tag{2}$$

where E is the associated electronic energy and $\hat{H}$ is the electronic Hamiltonian. In atomic units, the nonrelativistic spin- and field-free electronic Hamiltonian operator is given by Eqn (3):

$$\hat{H} = -\frac{1}{2}\sum_i \nabla_i^2 - \sum_{iK} \frac{Z_K}{|\mathbf{r}_i - \mathbf{R}_K|} + \sum_{i>j} \frac{1}{r_{ij}} + \sum_{K>L} \frac{Z_K Z_L}{R_{KL}} \tag{3}$$

where Z_K are the nuclear charges and where the summations are over all electrons i and all nuclei K. Because of boundary conditions, valid solutions Ψ do not exist for all energies E. In this paper, we are concerned with the ground-state wave function, associated with the lowest eigenvalue E.

All information about the electronic system is contained in the electronic wave function, obtained by solving the Schrödinger equation Eqn (2). Unfortunately, the Schrödinger equation represents a difficult many-body problem that cannot be solved exactly, see Plate 1. We are thus forced to make approximations in its solution, that is, to provide simplified descriptions that incorporate the most important features of the electronic system. This should preferably be done in an orderly fashion, so that the exact solution can be approached in a systematic manner. This particular approach to the molecular electronic many-body problem is discussed in this paper.

In passing, we note that a very different route to the many-body problem is provided by DFT.[5] In DFT, all information about the electronic system is extracted from the electron density (and possibly from the spin density) rather than from the wave function. Since, for any system, the electron density is a function of only three spatial coordinates, it is a much simpler function to approximate than the full electronic wave function, making DFT a highly attractive approach to the molecular many-body problem. Unfortunately, even though the electronic energy is a function of the electron density, in practice, this function is only known in a rather crude, approximate manner.[20] Moreover, no procedure has yet been developed for improving the approximate function in a systematic manner, making it impossible to refine our description of the molecular system towards the exact solution. The approach described here, in which we approximate the exact solution in a systematic manner, can therefore only be taken by resorting to wave-function theory and by attempting the difficult solution of the many-particle Schrödinger equation.

N-particle space and coupled-cluster theory

Hartree–Fock model and mean-field description. For a fictitious system of N non-interacting electrons, the exact wave function takes the form of a Slater determinant, that is, an antisymmetric product of N spin molecular orbitals (MOs) [Eqn (4)]:

$$\Phi = \hat{A}\prod_{I=1}^{N} \phi_I(\mathbf{x}_I), \langle \phi_I \mid \phi_J \rangle = \delta_{IJ} \tag{4}$$

In this expression, $\hat{A}$ is an antisymmetrizer (introduced to comply with the Pauli antisymmetry principle) and the $\phi_I(\mathbf{x})$ are a set of orthonormal one-electron functions

Copyright © 2004 John Wiley & Sons, Ltd.

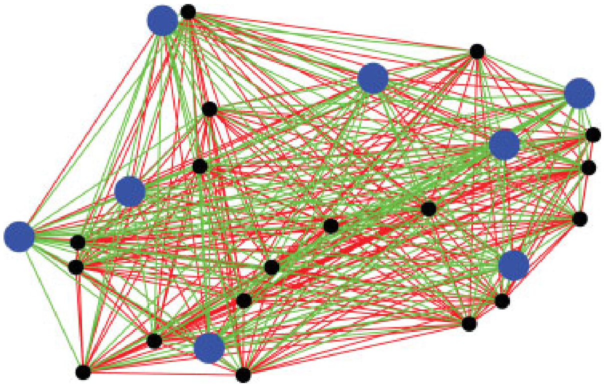

Plate 1. The molecular many-body problem. The nuclei and electrons are represented by large and small dots, respectively, and their interactions by straight lines

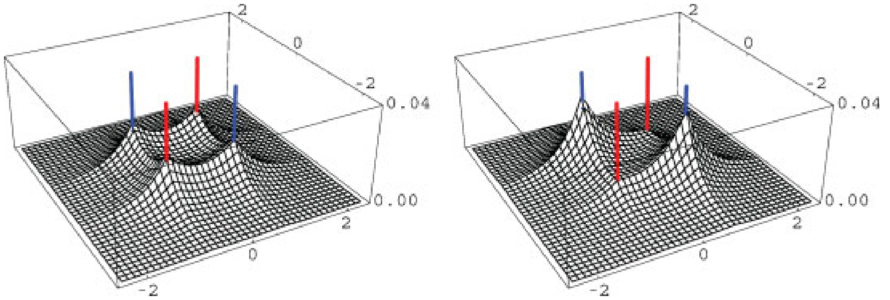

Plate 2. The two-electron density in H_2 with both electrons on the molecular axis. To the left, we have plotted the two-electron density of the uncorrelated Hartree–Fock state $|1\sigma_g^2\rangle$; to the right, we have plotted the density for the correlated state $|1\sigma_g^2\rangle - 0.11|1\sigma_u^2\rangle$ (atomic units). The red lines represent situations with both electrons at the same nucleus; the blue lines represent situations with the two electrons on opposite nuclei

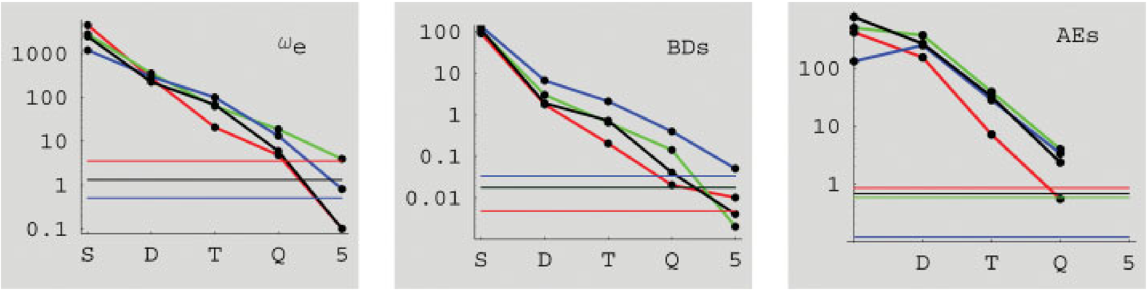

Plate 3. Errors in the calculated harmonic constants (cm^{-1}), bond distances (pm) and atomization energies (kJ mol^{-1}) of HF (red), CO (black), N_2 (green) and F_2 (blue), plotted on a logarithmic scale as functions of the highest included connected excitations in the coupled-cluster treatment. The straight lines represent the relativistic corrections

Copyright © 2004 John Wiley & Sons, Ltd.

(spin orbitals) of three spatial coordinates and one spin coordinate. In practice, each spin orbital is a product of a spatial, orbital part and one of the two possible spin functions α or β. For a closed-shell state, such as those considered here, the spin orbitals in the Hartree–Fock state Eqn (4) occur in pairs, with the same orbital part but different spin parts.

For a real system of interacting electrons, the exact wave function cannot be written in the product form Eqn (4). Still, we may take this particularly simple mathematical form as a useful *ansatz* for an approximate description of the electronic system. To make the most of this *ansatz* and generate the best possible ground-state determinantal wave function, we invoke the variation principle[19] and minimize the expectation value of the Hamiltonian with respect to the form of the MOs [Eqn (5)]:

$$E = \min_{\phi_I} \frac{\langle \Phi \,|\, \hat{H} \,|\, \Phi \rangle}{\langle \Phi \,|\, \Phi \rangle} \geq E_{\text{exact}} \tag{5}$$

subject to the constraint that the MOs remain orthonormal. This particular approach to the molecular many-body problem constitutes the Hartree–Fock model.[21]

In the Hartree–Fock description, each electron is described by taking into account only the mean effect of all other electrons, being affected by the average rather than instantaneous positions of the remaining electrons. Typical errors of the Hartree–Fock independent-particle model are 0.5% in the total energy, 1% in bond distances and 5–10% in many other molecular properties such as force constants and dipole moments.[1,22] However, for certain properties such as atomization energies and indirect nuclear spin–spin coupling constants, it may fail completely and give very large errors, see, for instance, Refs. 9 and 23.

The Hartree–Fock model is the cornerstone of molecular wave-function theory. It constitutes a useful, qualitative model on its own, applicable to large systems. More importantly, it forms the starting point for more accurate descriptions of molecular electronic systems, to which we now turn our attention.

Electron correlation and virtual excitations. Apart from obeying the Pauli antisymmetry principle, the mean-field Hartree–Fock description is uncorrelated. To improve upon this simple description, we must take into account the instantaneous interactions among the electrons. Thus, in real space, the electrons are constantly being scattered by collisions. In the orbital picture adopted by us, such collisions manifest themselves as virtual excitations from occupied spin orbitals $\phi_I(\mathbf{x})$ to virtual (unoccupied) spin orbitals $\phi_A(\mathbf{x})$.

The most important collisions are those between two electrons, corresponding to virtual excitations from two occupied to two virtual spin orbitals, known as pair excitations or double excitations. Let us represent the optimized Hartree–Fock state of Eqn (4) by $|\text{HF}\rangle$ and let $|IJ \rightarrow AB\rangle$ denote the doubly-excited state generated from $|\text{HF}\rangle$ by replacing spin orbitals I and J by spin orbitals A and B, respectively. Consider next the double-excitation operator $\hat{X}_{IJ}^{AB}$ that generates, from the Hartree–Fock state, this excited state, Eqn (6):

$$\hat{X}_{IJ}^{AB}|\text{HF}\rangle = t_{IJ}^{AB}|IJ \rightarrow AB\rangle \tag{6}$$

The amplitude t_{IJ}^{AB} that appears in this expression represents the probability that the two electrons in spin orbitals ϕ_I and ϕ_J will interact and as a result be excited to ϕ_A and ϕ_B. By applying $1 + \hat{X}_{IJ}^{AB}$ to the Hartree–Fock state, we generate an improved description of the electronic system [Eqn (7)]:

$$|\text{HF}\rangle \rightarrow (1 + \hat{X}_{IJ}^{AB})|\text{HF}\rangle \tag{7}$$

Our description of the electronic system is now said to be correlated, as opposed to the simple, uncorrelated description afforded by the mean-field Hartree–Fock model.

To illustrate the description of electron correlation by means of virtual excitations, consider the H_2 system in the basis of two Slater-type functions, one centered on each atomic nucleus [Eqn (8)]:

$$1s_{\text{A}} = \frac{1}{\sqrt{\pi}}\exp(-r_{\text{A}}),\, 1s_{\text{B}} = \frac{1}{\sqrt{\pi}}\exp(-r_{\text{B}}) \tag{8}$$

The two nuclei are located on the z axis at -0.7 and $0.7\,a_0$, respectively. From these atomic orbitals (AOs), we may generate two MOs [Eqn (9)]:

$$1\sigma_{\text{g}} = N_{\text{g}}(1s_{\text{A}} + 1s_{\text{B}}),\, 1\sigma_{\text{u}} = N_{\text{u}}(1s_{\text{A}} - 1s_{\text{B}}) \tag{9}$$

where N_{g} and N_{u} are normalization constants. In the Hartree–Fock ground-state description, the bonding $1\sigma_{\text{g}}$ orbital is doubly occupied and the antibonding $1\sigma_{\text{u}}$ orbital is unoccupied. By applying the operator $\hat{X}_{\text{gg}}^{\text{uu}}$, we obtain an improved description, where the electrons have a tendency to occupy the antibonding as well as the bonding orbital [Eqn (10)]:

$$|1\sigma_{\text{g}}^2\rangle \rightarrow (1 + \hat{X}_{\text{gg}}^{\text{uu}})|1\sigma_{\text{g}}^2\rangle = |1\sigma_{\text{g}}^2\rangle - 0.11|1\sigma_{\text{u}}^2\rangle \tag{10}$$

The amplitude -0.11 that occurs in this state has been obtained by a variational minimization of the expectation value of the electronic Hamiltonian.

As seen from Fig. 1, the one-electron density along the z axis $\rho(z)$ is hardly affected by correlation. By contrast, the two-electron density $\rho(z_1, z_2)$ along the same axis changes dramatically upon correlation, see Plate 2. In particular, along the diagonal $z_1 = z_2$, where the two electrons coincide, the two-electron density is strongly reduced. At the same time, there is an enhanced probability of finding the electrons on opposite sides of the system $z_1 = -z_2$, for example, on the two different nuclei.

Copyright © 2004 John Wiley & Sons, Ltd.

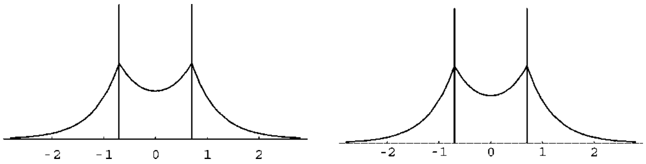

Figure 1. The one-electron density in H$_2$ on the molecular axis, plotted for the uncorrelated state $|1\sigma_g^2\rangle$ to the left and for the correlated state $|1\sigma_g^2\rangle - 0.11|1\sigma_u^2\rangle$ to the right (atomic units)

Coupled-cluster model. For an accurate description of the two-electron system, we must have a large set of AOs into which virtual excitations can occur, only in this manner will we be able to describe accurately the correlated motion between the two electrons as they approach each other in space. In addition, for systems containing more than two electrons, we cannot restrict ourselves to collisions between pairs of electrons and their representation in terms of double excitations. For high accuracy, we must also take into account processes that involve three or more electrons simultaneously. By a straightforward generalization of the approach for two electrons, we therefore introduce operators that carry out triple, quadruple and higher virtual excitations, with associated amplitudes [Eqns (11) and (12)]:

$$\hat{X}_{IJK}^{ABC}|\mathrm{HF}\rangle = t_{IJK}^{ABC}|IJK \rightarrow ABC\rangle \tag{11}$$

$$\hat{X}_{IJKL}^{ABCD}|\mathrm{HF}\rangle = t_{IJKL}^{ABCD}|IJKL \rightarrow ABCD\rangle \tag{12}$$

The final description is then obtained by applying, to the uncorrelated Hartree–Fock state, all possible combinations of such operators. The resulting wave function, in which there are no restrictions on the excitation operators that have been included, is the coupled-cluster representation of the full configuration–interaction (FCI) wave function [Eqn (13)]:[10]

$$\begin{aligned}|\mathrm{FCI}\rangle = &\left[\prod_{AI}\left(1+\hat{X}_I^A\right)\right]\left[\prod_{ABIJ}\left(1+\hat{X}_{IJ}^{AB}\right)\right] \\ &\times\left[\prod_{ABCIJK}\left(1+\hat{X}_{IJK}^{ABC}\right)\right]\cdots|\mathrm{HF}\rangle\end{aligned} \tag{13}$$

Because of the very large number of parameters involved in the construction of the FCI wave function, this approach can only be applied to small systems with small virtual excitation spaces.

For larger systems, we proceed by truncating the wave function, leaving out all excitation operators in Eqn (13) that involve more than a given number of electrons. For example, omitting all excitation operators that involve more than two electrons, we arrive at the coupled-cluster singles-and-doubles (CCSD) wave function [Eqn (14)]:[24]

$$|\mathrm{CCSD}\rangle = \left[\prod_{AI}\left(1+\hat{X}_I^A\right)\right]\left[\prod_{ABIJ}\left(1+\hat{X}_{IJ}^{AB}\right)\right]|\mathrm{HF}\rangle \tag{14}$$

Note carefully that, in the CCSD description, double excitations occur not only as a result of applying double-excitation operators to the Hartree–Fock state but also as a result of applying pairs of single-excitation operators. More generally, by expanding the CCSD state in Eqn (14), we obtain Eqn (15):

$$\begin{aligned}|\mathrm{CCSD}\rangle = {} & |\mathrm{HF}\rangle + \sum_{AI}\hat{X}_I^A|\mathrm{HF}\rangle + \sum_{ABIJ}(\hat{X}_{IJ}^{AB} + \hat{X}_I^A\hat{X}_J^B)|\mathrm{HF}\rangle \\ & + \sum_{ABCIJK}(\hat{X}_I^A\hat{X}_{IJ}^{BC} + \hat{X}_I^A\hat{X}_J^B\hat{X}_K^C)|\mathrm{HF}\rangle \\ & + \sum_{ABCDIJKL}(\hat{X}_{IJ}^{AB}\hat{X}_{KL}^{CD} + \hat{X}_I^A\hat{X}_J^B\hat{X}_{KL}^{CD} + \hat{X}_I^A\hat{X}_J^B\hat{X}_K^C\hat{X}_L^D)|\mathrm{HF}\rangle + \cdots\end{aligned} \tag{15}$$

where, for example, $\hat{X}_{IJ}^{AB}|\mathrm{HF}\rangle$ is known as a connected cluster and $\hat{X}_I^A\hat{X}_J^B|\mathrm{HF}\rangle$ as a disconnected one. Clearly, in the CCSD state, all clusters involving three or more electrons are disconnected, representing two or more independent virtual excitations in the electronic system, for example, two separate, independent double excitations $\hat{X}_{IJ}^{AB}\hat{X}_{KL}^{CD}|\mathrm{HF}\rangle$. In real space, such disconnected quadruple excitations correspond to two separate collisions, each involving two electrons. It is the compact description of such disconnected processes (as products) that constitutes the key to the success of coupled-cluster theory in quantum chemistry and that distinguishes it from the much less successful truncated configuration–interaction (CI) theory,[25] where all virtual excitations are either described totally in terms of connected clusters or else not described at all. For example, in the CI singles-and-doubles (CISD) model, we ignore all virtual excitations higher than the double excitations, arriving at the following wave function [Eqn (16)]:

$$|\mathrm{CISD}\rangle = |\mathrm{HF}\rangle + \sum_{AI}C_I^A|I \rightarrow A\rangle + \sum_{ABIJ}C_{IJ}^{AB}|IJ \rightarrow AB\rangle \tag{16}$$

Since the CISD model ignores all excitations involving more than two electrons (even the dominant disconnected excitations), it works much better for small electronic

Copyright © 2004 John Wiley & Sons, Ltd.

systems, where disconnected excitations are less important, than in larger systems. By contrast, the truncated coupled-cluster model in Eqs (14) and (15) works equally well for small and large systems, owing to its ability to describe simultaneous but independent virtual excitations as products of connected clusters.

At the limit of no truncation, the coupled-cluster wave function Eqn (13) becomes equivalent to the CI wave function without truncation, that is, to the FCI wave function [Eqn (17)]:

$$|\mathrm{FCI}\rangle = |\mathrm{HF}\rangle + \sum_{AI} C_I^A |I \to A\rangle + \sum_{ABIJ} C_{IJ}^{AB} |IJ \to AB\rangle + \sum_{ABCIJK} C_{IJK}^{ABC} |IJK \to ABC\rangle + \cdots \quad (17)$$

At this limit, the coupled-cluster and CI wave functions differ only in their parameterization and, in this special case, the simple linear CI parameterization Eqn (17) is preferable to the more complicated nonlinear coupled-cluster parameterization Eqn (13).

Coupled-cluster hierarchy of wave functions. By truncating the FCI expansion in the coupled-cluster representation Eqn (13) at different excitation levels, we arrive at the standard coupled-cluster hierarchy of wave functions. At the lowest level of this hierarchy, we have the uncorrelated Hartree–Fock model, with no virtual excitations. Next, by allowing all single excitations to occur out of the Hartree–Fock state, we obtain the coupled-cluster singles (CCS) description. However, because of the variational property of the Hartree–Fock state Eqn (5), the singles amplitudes in the CCS wave function are all zero, making this level of theory of no interest to us here[1] (although it does play a role in the calculation of some molecular properties[26]). Therefore, the first nontrivial coupled-cluster model is the CCSD model Eqn (14), in which all possible single and double excitation operators are included. We note that, because of the presence of the double excitations, the single-excitation amplitudes are non-zero in the CCSD wave function, unlike in the CCS wave function.

At the CCSD level of theory, we describe the most important virtual processes in the electronic system, that is, all virtual double excitations and all products of such excitations. At this level of theory, the errors in the electronic energy and in other molecular properties are typically reduced by a factor of three or four relative to the Hartree–Fock description. This is obviously a significant improvement on our original description but it is rarely sufficient for a quantitative description of the molecular system.

At the next level of approximation, we introduce connected triple excitations, thereby arriving at the coupled-cluster singles-doubles-and-triples (CCSDT) model.[27,28] At this level of theory, the errors are reduced by a further factor of three or four, which means that the CCSDT model is about an order of magnitude more accurate than the Hartree–Fock model. Indeed, this accuracy is often but by no means always sufficient for a full agreement with measurements (within experimental error bars).[29] If not, further improvements are possible, in principle, at least, if not always in practice, by including in our description the connected quadruple excitations at the CCSDTQ level of theory,[30] the connected quintuple excitations at the CCSDTQ5 level of theory,[31] and so on.

Because of the complexity of the coupled-cluster wave function, it is usually not determined variationally (i.e. by minimizing the expectation value of the Hamiltonian) but rather by a related nonvariational projection technique,[1] which we do not describe here except to note that the energy does become variational in the FCI limit. As a result, the truncated coupled-cluster energy does not constitute a strict upper bound to the exact energy. In practice, this does not matter much since the coupled-cluster energy is anyway a rather accurate, small correction to the Hartree–Fock electronic energy (which does represent an upper bound) and since the coupled-cluster energy does approach the variational FCI energy as progressively higher-order excitations are included in the description.

Although the coupled-cluster hierarchy converges fairly rapidly with the increasing excitation level (with about an order of magnitude higher accuracy gained at every second level), it rapidly becomes expensive.[10] Formally, the cost of the coupled-cluster model is proportional to K^{2m+2}, where K is the number of atoms (as a measure of the size of the system) and m is the order of the highest connected clusters included in the description ($m = 2$ for CCSD, $m = 3$ for CCSDT, etc.). In practice, this means that we can apply the CCSD model to rather large systems, containing tens of atoms, but that the CCSDT model is too expensive for systems containing more than a few atoms. We note, however, that with the recent developments in linear-scaling techniques,[12–18] the cost is dramatically reduced for large systems, making it possible to carry out coupled-cluster calculations on large molecules.[17]

Perturbative treatments of the coupled-cluster amplitudes. To reduce the cost and thereby extend the application range of coupled-cluster theory, the amplitudes of the cluster operators are sometimes determined not by projection (which is an iterative process) but by a non-iterative perturbation technique. At the lowest level of approximation, this approach leads to the second-order Møller–Plesset (MP2) model,[1] which could be viewed as a perturbative alternative to the CCSD model. However, a fundamental problem with the Møller–Plesset perturbation expansion is that, taken to sufficiently high orders, it usually diverges, that is, unlike the pure coupled-cluster method, it does not approach the FCI limit as the description is refined.[32,33]

Copyright © 2004 John Wiley & Sons, Ltd.

In general, therefore, perturbation theory does not constitute a useful alternative to coupled-cluster theory when high accuracy is essential. Still, it is sometimes a good idea to determine not all coupled-cluster amplitudes but only those that characterize the highest connected virtual excitations by perturbation theory. Thus, at the CCSD(T) level of theory, we generate the connected single and double amplitudes in the usual projective manner of coupled-cluster theory but determine the more expensive connected triple amplitudes by perturbation theory.[34] In this manner, the overall cost is reduced from K^8 for CCSDT to K^7 for CCSD(T).[10] Moreover, whereas the CCSD(T) single and double amplitudes are determined iteratively at cost K^6, the K^7 cost of the perturbative triples is non-iterative. As we shall see, this technique expands the application range of calculations with connected triples significantly, introducing an error of about 10% in the triples description. However, since the connected triples represent a rather small correction to the CCSD description, this error is of little significance. Moreover, the error incurred by the perturbation treatment of the triples (as opposed to the full coupled-cluster treatment) is usually such that it cancels, to some extent, the error incurred by omitting the connected quadruples and higher excitations from our description. In fact, as a result of this error cancellation, the CCSD(T) model often performs better than the more expensive CCSDT model; see, for instance, Ref. 35.

In a similar manner, we may view the inexpensive MP2 model (cost K^5) as an approximation to the CCSD model (cost K^6) where the highest-order amplitudes are determined by perturbation theory. Again, there is an element of error cancellation in the MP2 model that often compensates for its cruder description of the electronic structure, making it an inexpensive and useful but somewhat erratic alternative to the CCSD model.[1]

Example: the coupled-cluster calculation of the atomization energy of CO. To illustrate the convergence of the coupled-cluster hierarchy, we consider the calculation of the atomization energy of CO. In Table 1, we have listed the contributions to the atomization energy at different levels of coupled-cluster theory. The atomization energy is obtained by subtracting the energy of CO from the sum of the energies of the constituent atoms; in the table, the molecular and atomic energies are listed separately.

Table 1. Calculation of the atomization energy of the CO molecule (kJ mol^{-1}). All calculations have been carried out at the optimized CCSD(T)/cc-pCVQZ bond distance of 112.9 pm.[8] The experimental atomization energy is 1071.8 kJ mol^{-1} (see Table 7)

	E_{C}	+	E_{O}	−	E_{CO}	=	D_{CO}	Error
HF	−98964.9	−	196437.1	+	296132.2	=	730.1	−341.7
SD	−388.4	−	639.6	+	1350.2	=	322.1	−19.6
(T)	−7.7	−	11.9	+	54.2	=	34.6	15.0
Vib.	0.0	+	0.0	−	12.9	=	−12.9	2.1
Rel.	−40.1	−	139.0	+	177.1	=	−2.0	−0.1
Total	−99401.1	−	197227.6	+	297700.8	=	1071.9	

We first note that the atomization energy constitutes less than 1% of the total electronic energy. Clearly, for chemical accuracy in the calculated atomization energy [i.e. error less than about 1 kcal mol^{-1} (1 kcal = 4.184 kJ)], the separate atomic and molecular contributions must be calculated to a high precision. Moreover, upon atomization, the electronic structure changes dramatically from a strongly correlated closed-shell molecular system consisting of paired valence electrons to a weakly correlated open-shell atomic system containing unpaired valence electrons. Therefore, for a quantitative treatment of such processes, electron correlation must be described accurately. Thus, whereas the Hartree–Fock model contributes 99.5% of the total electronic energy of CO, it contributes only 67% to the atomization energy. Similarly, the doubles contribute only 0.5% to the energy of CO but 30% to the atomization energy, whereas the triples contribute a minute 0.01% to the total energy but as much as 3% to the atomization energy of CO.

Nevertheless, the coupled-cluster convergence is rapid, the error being reduced by an order of magnitude with each new excitation level. Indeed, at the CCSD(T) level of theory, the contributions from molecular vibrations and from relativity appear to be more important than the contributions from the neglected higher-order excitation levels. We shall return to this point later, when we examine the calculation of atomization energies more closely under the section on Atomization energies. At present, we are content to observe that the coupled-cluster hierarchy does seem to work and turn our attention instead to an important point that we have so far glossed over: the basis-set requirements of coupled-cluster theory. We note that the results in Table 1 are definite in the sense that they correspond to those obtained in an infinitely large basis set (i.e. in a complete virtual excitation space). In a finite basis, very different values are obtained, as we shall see shortly.

One-particle space and correlation-consistent basis sets

Gaussian basis functions. The many-electron wave functions discussed in this paper are expanded in a set of orthonormal one-electron functions or molecular orbitals (MOs): the occupied MOs and the virtual MOs. The occupied MOs are those from which the Hartree–Fock wave function Eqn (4) is constructed; the virtual MOs are those into which electrons are excited in the coupled-cluster wave function Eqn (14). Each of these MOs is constructed from a set of atomic orbitals (AOs), which are usually taken to be a finite set of simple analytical functions, centered on the atomic nuclei,[1] typically fixed combinations of Gaussian orbitals of the form in Eqn (18):[36]

$$G_{ijk}(r_A, \alpha) = x_A^i y_A^j z_A^k \exp(-\alpha r_A^2) \tag{18}$$

where i, j and k are non-negative integers, α is a positive real number, and $\mathbf{r}_A$ is the position of the electron relative to nucleus A. Letting $\phi_p(\mathbf{r})$ be the spatial part of the spin orbital $\phi_P(\mathbf{x})$, we expand this MO as Eqn (19):

$$\phi_p(\mathbf{r}) = \sum_{\mu} C_{\mu p} \chi_\mu(\mathbf{r}) \tag{19}$$

where the $\chi_\mu(\mathbf{r})$ are the AOs. For an accurate description of the electronic system, we must have a large set of such AOs to ensure an accurate representation of the occupied MOs and also to create a large virtual space so as to recover a large proportion of the correlation energy, which is here taken to be the difference between the exact non-relativistic energy in a complete one-electron basis and the Hartree–Fock energy in the same basis.

In molecular calculations, the wave function is constructed from standard collections or sets of atom-centered AOs, obtained from atomic calculations.[37,38] The question then arises as to what AOs should be included in the basis set so as to provide an optimal description of the electronic system for a given number of AOs. It turns out that the basic principles underlying the construction of basis sets for correlation energies can be learned from studies of the ground-state two-electron helium atom.

Principal expansion and explicitly correlated methods. From calculations on the helium atom, it is known that each atomic orbital makes a contribution to the correlation energy that, to a good approximation, depends only on its principal quantum number n and is proportional to n^{-6} [Eqn (20)]:[39,40]

$$\varepsilon_{nlm} \propto n^{-6} \tag{20}$$

In other words, all orbitals that belong to the same shell contribute the same amount of correlation energy. This observation leads us to the concept of the principal expansion, according to which we include in our description all AOs belonging to the same shell simultaneously, in order of increasing quantum number n.[1] Since each added shell contains n^2 orbitals, it contributes the amount of correlation energy shown in Eqn (21):

$$\varepsilon_n \propto n^2 n^{-6} = n^{-4} \tag{21}$$

thereby ensuring the fastest possible convergence to the basis-set limit of the correlation energy (i.e. to the correlation energy in the limit of a complete set of orbitals).

Let us now assume that we have carried out a calculation on the helium atom where we have included all shells $n \leq X$, where X is known as the cardinal number of the basis set. We first note that the number of AOs in the basis set is proportional to the cardinal number cubed [Eqn (22)]:

$$N_X = \sum_{n=1}^{X} n^2 \propto X^3 \tag{22}$$

Next, we estimate the error in the correlation energy by adding together the contributions from all omitted shells [Eqn (23)]:

$$\Delta E_X \propto \sum_{n=X+1}^{\infty} n^{-4} \propto X^{-3} \tag{23}$$

This result shows that the error in the correlation energy is inversely proportional to the cardinal number cubed and inversely proportional to the total number of AOs $\Delta E_X \propto N_X^{-1}$.[41] This convergence is slow indeed, as illustrated in Fig. 2, where we have plotted the error in the energy (on a logarithmic scale) as a function of the number of determinants in the FCI expansion of the wave function. As this plot shows, it is exceedingly difficult to calculate the energy to an accuracy of $1\,\mathrm{m}\ E_\mathrm{h} = 2.625\,\mathrm{kJ\,mol^{-1}}$ (chemical accuracy) by coupled-cluster theory, when the wave function is expanded in products of orbitals as in Eqn (13).

The slow convergence of the correlation energy in helium arises from a poor description of short-range (dynamic) correlation in the orbital approximation.[1] This deficiency of the orbital expansion is illustrated in Fig. 3, where we have plotted the wave function on a circle of radius 0.5 a_0 about the nucleus, with one electron fixed at the origin of the plot. Whereas the first derivative of the exact wave function changes sign discontinuously at the point of coalescence, the approximate orbital-based wave function changes smoothly

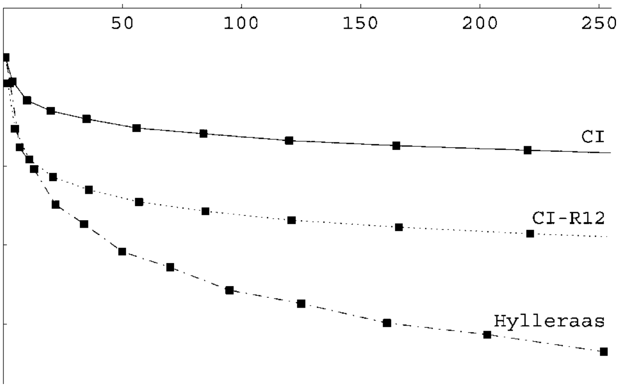

Figure 2. Error in the energy of the ground-state helium atom (E_h) on a logarithmic scale as a function of the number of included terms in the standard CI expansion, in the CI–R12 expansion, and in the Hylleraas expansion

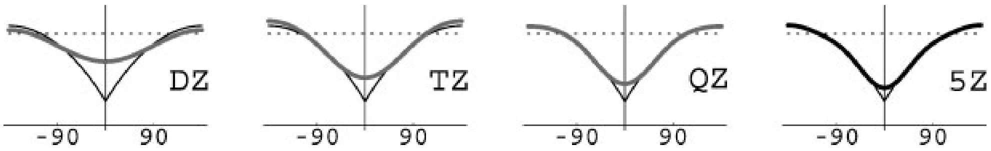

Figure 3. The ground-state helium wave function plotted on a circle of radius $0.5a_0$ about the nucleus with one electron fixed at the origin of the plot. The dotted and full black lines represent the Hartree–Fock and Hylleraas wave functions, respectively. The full grey lines represent the FCI wave functions generated using the correlation-consistent basis sets cc-pV*XZ*

and overestimates the probability of coalescence, for all cardinal numbers.

To improve basis-set convergence and provide a correct description of the wave function at small interelectronic distances, we can use explicitly correlated wave functions, where the interelectronic distances r_{ij} are used as variables.[1] In Fig. 2, we have plotted the error in the energy for wave functions where the r_{12} term is included linearly (CI–R12) and to arbitrary powers (the Hylleraas function). Clearly, the explicitly correlated methods, in particular, the Hylleraas expansion,[42] converge much more rapidly to the basis-set limit than does the orbital-based expansion. Whereas the generalization of the Hylleraas wave function to molecular systems has proved very difficult, the linear R12 method has been generalized to such systems in the form of MP2-R12[43] and CCSD-R12[44] theories and is used on several occasions in this paper for benchmarking of the standard orbital-based coupled-cluster method.

Correlation-consistent basis sets. A practical realization of the principal expansion for many-electron systems are the correlation-consistent basis sets.[45–48] In these basis sets, atomic energy-optimized orbitals are added to the basis, one shell at a time in the sense of the principal expansion, so as to ensure the fastest possible convergence of the correlation energy to the basis-set limit. The series begins with the correlation-consistent valence double-zeta basis set cc-pVDZ, of cardinal number $X = 2$ and with 14 AOs of composition 3s2p1d for first-row atoms such as carbon. Increasing the cardinal number, we have the triple-zeta cc-pVTZ basis set with 30 AOs of composition 4s3p2d1f, the quadruple-zeta cc-pVQZ basis sets with 55 AOs of composition 5s4p3d2f1g, and so on. In general, the cc-pV*XZ* basis of cardinal number X contains $\frac{1}{3}(X+1)(X+\frac{3}{2})(X+2)$ AOs.

The correlation-consistent cc-pV*XZ* basis sets are designed for correlation of the valence electrons, which is often sufficient for a qualitative description of the electronic system (noting that most chemical processes involve mainly rearrangements of the electronic structure in the valence region). However, for an accurate description of chemical processes, it is usually necessary to correlate all the electrons, even those in the core. For such calculations, the correlation-consistent core–valence cc-pCV*XZ* basis sets have been developed,[49,50] in which the cc-pV*XZ* basis sets are augmented with compact Gaussians (i.e. Gaussians with large exponents). Likewise, for a flexible description of the outer valence region, we can use the aug-cc-pV*XZ* or aug-cc-pCV*XZ* basis sets,[47,51] where diffuse functions (i.e. Gaussians with small exponents) have been added. For an overview over the correlation-consistent basis sets, see Table 2.

To illustrate the convergence of the correlation energy with the cardinal number, we have, in Table 3, listed the contributions to the atomization energy of CO for different core–valence basis sets. As expected, the correlation energy converges very slowly, in particular, for the dominant double excitations. In fact, chemical accuracy (i.e. an error of the order of $1\,\mathrm{kcal\,mol^{-1}}$) requires a total of 230 AOs on each atom. We note, however, that the Hartree–Fock and triple-excitation contributions are less of a problem, converging to chemical accuracy much earlier.

Basis-set extrapolation. Although the convergence of the correlation energy with respect to the cardinal number is excruciatingly slow, it is at the same time smooth. In particular, from our discussion of the principal expansion, we expect the correlation energy calculated with cardinal number X to be related to the correlation energy in the basis-set limit as in Eqn (24):

$$E_\infty = E_X + AX^{-3} \tag{24}$$

Table 2. Composition of the correlation-consistent valence cc-pV*XZ* basis sets with N_V AOs for first-row atoms, the core–valence cc-pCV*XZ* basis sets with N_CV AOs, and the augmented basis sets aug-cc-pV*XZ* basis sets with N_aug AOs

X	cc-pV*XZ*	N_V	cc-pCV*XZ*	N_CV	aug-cc-pV*XZ*	N_aug
D	3s2p1d	14	+ 1s1p	18	+ 1s1p1d	23
T	4s3p2d1f	30	+ 2s2p1d	43	+ 1s1p1d1f	46
Q	5s4p3d2f1g	55	+ 3s3p2d1f	84	+ 1s1p1d1f1g	80
5	6s5p4d3f2g1h	91	+ 4s4p3d2f1g	145	+ 1s1p1d1f1g1h	127

Copyright © 2004 John Wiley & Sons, Ltd.

Table 3. Basis-set convergence of the different CCSD(T) contributions to the electronic part of the atomization energy of CO (kJ mol^{-1}), calculated at the CCSD(T)/cc-pCVQZ bond distance of 112.9 pm

	N_{bas}	HF		SD		(T)		CCSD(T)	Error
cc-pCVDZ	36	710.2	+	277.4	+	24.5	=	1012.1	−74.8
cc-pCVTZ	86	727.1	+	297.3	+	32.6	=	1057.0	−29.9
cc-pCVQZ	168	730.3	+	311.0	+	33.8	=	1075.1	−11.8
cc-pCV5Z	290	730.1	+	316.4	+	34.2	=	1080.7	−6.2
cc-pcV6Z	460	730.1	+	318.8	+	34.4	=	1083.3	−3.6
Limit	∞	730.1	+	322.1	+	34.6	=	1086.9	0.0

Carrying out two different calculations with cardinal numbers X and $X-1$, we can eliminate A from this equation to obtain the two-point extrapolation formula in Eqn (25) for the correlation energy in the basis-set limit:[52,53]

$$E_{\infty} = \frac{X^3 E_X - (X-1)^3 E_{X-1}}{X^3 - (X-1)^3} \tag{25}$$

To illustrate the usefulness of this formula, in Table 4 we have listed the errors in the electronic energy with and without extrapolation. At the triple-zeta level, extrapolation reduces the error in the energy by a factor of three; for higher cardinal numbers, the error is reduced by an order of magnitude. Applied to the atomization energy of CO, we now find that chemical accuracy is achieved with just 168 AOs at the cc-pCV(TQ)Z level of theory, at a fraction of the cost, see Table 5. The notation cc-pCV(TQ)Z is used here for results obtained by applying the two-point extrapolation formula Eqn (25) to the results obtained separately with the cc-pCVTZ and cc-pCVQZ basis sets.

Two-dimensional chart of orbital-based quantum chemistry

We have seen that the quality of quantum-chemical calculations are determined by, on the one hand, the description of the N-electron space (the wave-function model) and, on the other hand, the quality of the one-electron space (basis set). More specifically, in orbital-based coupled-cluster theory, the accuracy is determined by the excitation level of the calculation, which determines the highest connected excitations included in the wave function, and by the cardinal number, which determines the flexibility of the virtual excitation space. To approach the exact solution, we must increase, in some systematic manner, both the excitation level and the cardinal number, see Fig. 4, which constitutes the two-dimensional chart of orbital-based quantum chemistry. Moreover, such extensions should be carried out in a balanced manner. Thus, for high accuracy, it is useless to increase the excitation level to include all electrons if the cardinal number is kept equal to two. Conversely, high accuracy cannot be achieved by increasing the cardinal number to achieve basis-set convergence if no higher than connected double excitations are allowed in our description. In the next section, we shall explore the two-dimensional chart of Fig. 4, so as to develop an understanding of what levels of theory are necessary to achieve a given level of accuracy in non-relativistic orbital-based quantum chemistry.

Table 4. Mean absolute errors (mE_h) in the calculated CCSD(T)/cc-pCVXZ electronic energies[a] of CH_2, H_2O, HF, N_2, CO, Ne and F_2 relative to experimental energies.[b] The extrapolated energies have been obtained from the plain energies by using Eqn (25)

	DZ	TZ	QZ	5Z	6Z	R12
Plain	194.8	62.2	23.1	10.6	6.6	1.4
Extr.		21.4	1.4	0.4	0.5	

[a] All calculations have been carried out at the optimized all-electron CCSD(T)/cc-pCVQZ geometry.

[b] The experimental energies have been obtained from experimental dissociation energies and estimated total atomic energies as discussed in Ref. 54.

Table 5. Basis-set errors in the atomization energy of CO (kJ mol^{-1}), calculated at the CCSD(T)/cc-pCVXZ level of theory relative to the R12 method. The extrapolated CCSD(T) energies have been obtained from the plain energies by using Eqn (25)

	DZ	TZ	QZ	5Z	6Z
Plain	−73.5	−28.3	−11.4	−6.0	−3.5
Extr.		−18.5	−0.7	0.0	0.0

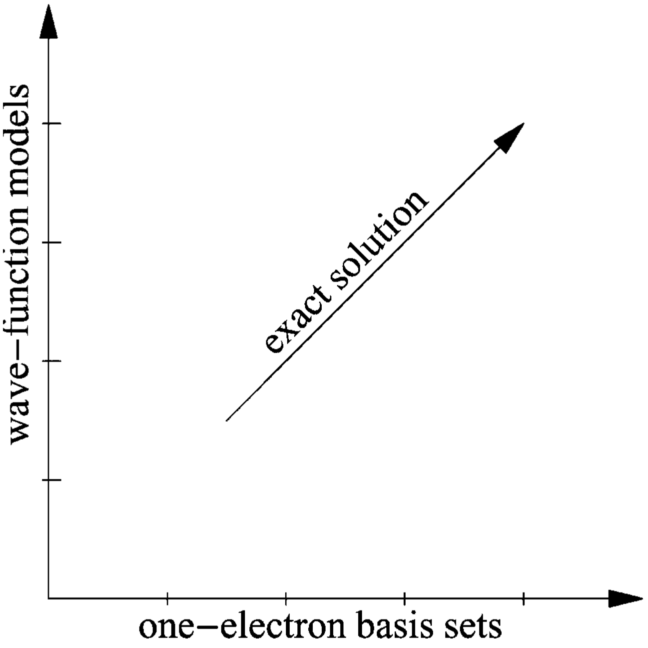

Figure 4. Two-dimensional chart of quantum chemistry

Copyright © 2004 John Wiley & Sons, Ltd.

APPLICATIONS

Having outlined the theory of orbital-based coupled-cluster theory in the previous section, we now go on to apply this theory to the calculation of some properties of molecular systems and their reactions, such as atomization energies, reaction enthalpies, bond distances and vibrational spectroscopic constants. For all properties, our emphasis is on what level of theory in the two dimensional chart of Fig. 4 is needed to achieve an accuracy in the calculations comparable to that of experimental measurements (chemical accuracy). We shall pay special attention to one particularly troublesome aspect of quantum-chemical calculations: namely, cancellation of errors, which often leads to a fortuitous agreement with experimental measurements. Whenever possible, we shall aim to avoid such (often erratic) cancellations, thereby arriving at the 'right answer for the right reason'.

Atomization energies

In this section, we consider the equilibrium atomization energy, which, for a given molecule, represents the difference between the energy of its constituent atoms in their electronic ground-state level $E^A(^{2S+1}L)$ and the molecular equilibrium ground-state electronic energy $E(\mathbf{R}_e)$ [Eqn (26)]:

$$D_e = \sum_A E^A(^{2S+1}L) - E(\mathbf{R}_e) \qquad (26)$$

We carried out comparisons with experiment (corrected for vibrations and relativity) at various levels of theory for the 17 closed-shell organic molecules listed in Table 7 (except HOF, which has been omitted for reasons explained later).[8] All calculations were carried out at the optimized all-electron CCSD(T)/cc-pCVQZ equilibrium geometry.

Since electron pairs are broken upon atomization, the atomization energy is a difficult property to calculate precisely, requiring an accurate treatment of electron correlation as noted in our discussion of the atomization energy of CO. The Hartree–Fock model, which ignores the effects of electron correlation, therefore performs very poorly, underestimating atomization energies by typically 40%. In Fig. 5, where we have plotted the mean errors and standard deviations in the atomization energies relative to experiment, the Hartree–Fock values have therefore been omitted so that the details in the performance of the more accurate MP2, CCSD and CCSD(T) models are not lost.

From Fig. 5, we note that the atomization energies increase with the cardinal number, for all *N*-electron models. This systematic behavior can be understood from the more general observation that, with an increase in the basis set, the energy is always lowered most for systems of low electronic energy,[1] that is, the difference in the energy between two systems (such as a molecule and its constituent atoms) always increases upon basis-set extension.

Next, concerning the *N*-electron description, we note that atomization energies in general increase with increasing excitation level in the coupled-cluster hierarchy: HF < CCSD < CCSD(T) < MP2. The failure of the MP2 model to fit this simple scheme follows from the fact that its double excitation amplitudes are determined perturbatively, which typically leads to an overestimation of the amplitudes relative to a full CCSD treatment.

In passing, we note the error cancellation at the MP2/cc-pCVTZ level of theory in Fig. 5. In general, such error cancellations, which are ubiquitous in quantum chemistry, occur since the errors arising from a poor *N*-electron description (here the approximate treatment of the doubles) and from the use of a too small basis set (here a triple-zeta basis) are often of opposite signs. Consequently, any improvement either in the *N*-electron description or in the one-electron description will typically result in a poorer agreement with experiment. Computational models with large error cancellations should therefore either be avoided or at least be treated with caution.

Concerning the agreement with experiment, we note that the mean absolute cc-pcV6Z errors are 423.0, 36.2, 37.2 and 4.6 kJ mol^{-1}, respectively, at the Hartree–Fock, MP2, CCSD and CCSD(T) levels of theory.[8] (The cc-pcV6Z results were obtained from the valence-electron

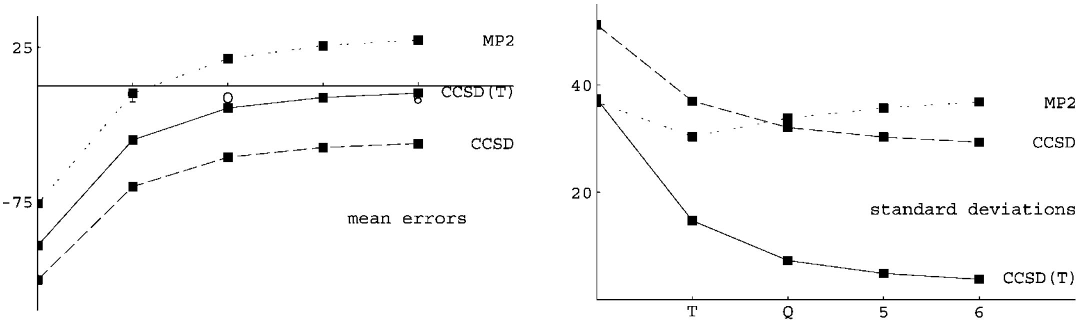

Figure 5. Mean errors and standard deviations relative to experiment in all-electron calculations of atomization energies (kJ mol^{-1}) in the cc-pCV*X*Z basis sets with $2 \leq X \leq 6$

Copyright © 2004 John Wiley & Sons, Ltd.

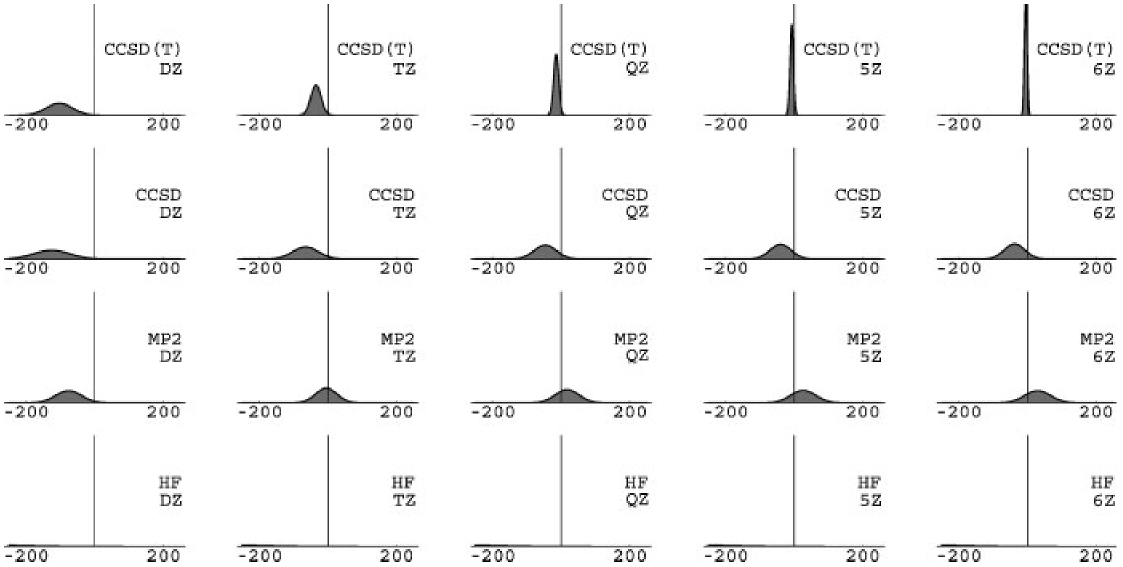

Figure 6. Normal distributions of errors in atomization energies (kJ mol^{-1}), calculated with all electrons correlated

cc-pV6Z results, with core corrections calculated in the cc-pCV5Z basis.) Clearly, the CCSD(T) model is the only model capable of chemical accuracy, although we note that the double- and triple-zeta basis sets are too small, the CCSD(T)/cc-pCV*X*Z mean errors being −103.3, −34.9, −14.3, −7.4 and −4.6 kJ mol^{-1}, respectively, for $2 \leq X \leq 6$.[8] These relationships are visualized in Fig. 6, where we have plotted the normal distributions of the errors in the calculated atomization energies relative to experiment. Clearly, to take full advantage of the CCSD(T) model, basis sets of at least cc-pCVQZ quality should be used, CCSD(T)/cc-pCVDZ calculations being meaningless except for comparison with models that include higher excitation levels.

In the section on the one-particle space and correlation-consistent basis sets, we saw that the calculated atomization energies converge very slowly to the basis-set limit because of errors in the description of short-range interactions. To accelerate convergence, we may apply the two-point extrapolation formula Eqn (25). As seen from Table 6, chemical accuracy is now achieved with the cc-pCVQZ basis. In Fig. 7, we plotted the normal distributions with and without such extrapolations, illustrating the dramatic improvement in the accuracy of the calculated atomization energies observed upon extrapolation. The two-point extrapolation is used in the W1 method of Martin and co-workers[55,56] and included in Gaussian 03.[57]

Table 6. Mean errors in the CCSD(T)/cc-pCV*X*Z atomization energies (kJ mol^{-1}) relative to experiment. The extrapolated atomization energies were obtained from the plain energies by using Eqn (25)

	DZ	TZ	QZ	5Z	6Z
Plain	−103.3	−34.9	−14.3	−7.4	−4.7
Extr.		−16.2	−1.1	−0.6	−0.9

In Table 7, calculated and experimental atomization energies, corrected for the effects of relativity and vibrational motion, are listed. In the largest basis set, the errors in the calculated atomization energies are larger than 2.2 kJ mol^{-1} only for O_3 and HOF. While the discrepancy for O_3 arises from an inadequate treatment of the multiconfigurational electronic structure of this molecule at the CCSD(T) level of theory, the discrepancy for HOF is related to an error in the NIST–JANAF tables.[58] Because of this error, HOF was omitted from our statistical analysis.

Since most of the changes in the electronic structure of a molecular system upon atomization occur in the valence region, it is tempting to calculate the atomization energies by ignoring core correlation. Still, for agreement with experiment to within chemical accuracy, core correlation cannot be neglected, contributing as much as 4.8 kJ mol^{-1} for CO and 10.8 kJ mol^{-1} for C_2H_2.[1] These core contributions were estimated in the cc-pCV5Z basis, by comparing the atomization energies obtained with and without core correlation.

To some extent, the excellent performance of the CCSD(T) model observed in Table 7 arises from error cancellation.[29] As seen from Table 8, relaxation of the triples contribution from the perturbative treatment at the CCSD(T) level to the full coupled-cluster treatment at the CCSDT level reduces the atomization energies, making the agreement with experiment poorer.[35] However, inclusion of the quadruples in the CCSDTQ model increases the atomization energies again, making the agreement even better than at the CCSD(T) level of theory.[29] We conclude that the rigorous calculation of atomization energies to chemical accuracy requires a treatment of the electronic structure at the CCSDTQ/cc-pCV6Z level of theory.

The error in the CCSD(T) triples contribution incurred by treating the connected triples by perturbation theory is fairly large (about 10% of the full triples contribution) but

Copyright © 2004 John Wiley & Sons, Ltd.

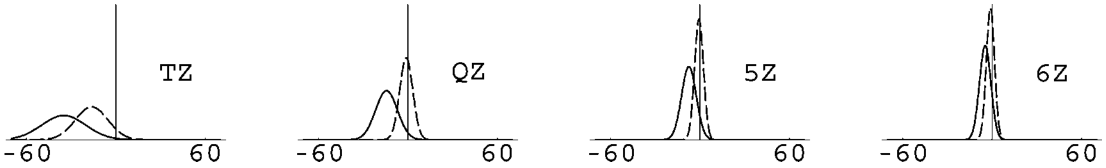

Figure 7. Normal distributions of the errors in the calculated all-electron CCSD(T)/cc-pCV*X*Z atomization energies (kJ mol^{-1}) without extrapolation (full line) and with two-point extrapolation (dotted line)

Table 7. Non-relativistic calculated and experimental electronic atomization energies with calculated vibrational and relativistic corrections[a] (kJ mol^{-1}). The Hartree–Fock atomization energies were calculated in the cc-pV6Z basis; the correlated atomization energies were calculated with two-point extrapolation, at the all-electron cc-pcV(56)Z level. All calculations were carried out at the optimized all-electron CCSD(T)/cc-pCVQZ geometry

	Non-relativistic electronic atomization energy						
Molecule	HF	MP2	CCSD	CCSD(T)	Exp.	Vib. corr.	Rel. corr.
F_2	−155.3	185.4	128.0	161.1	163.4(06)	−5.5	−3.3
H_2	350.8	440.7	458.1	458.1	458.0(00)	−26.0	0.0
HF	405.7	613.8	583.9	593.3	593.2(09)	−24.5	−2.5
O_3	−238.2	726.6	496.1	605.5	616.2(17)	−17.4	−3.9
HOF	230.4	695.0	627.5	662.9	674.9(42)	−35.9	−3.5
$CH_2(^1A_1)$	531.1	740.8	749.4	757.9	757.1(22)	−43.2	−0.7
HNO	331.6	897.2	816.8	860.4	861.5(03)	−35.8	−2.1
N_2	482.9	1010.6	913.9	954.9	956.3(02)	−14.1	−0.6
H_2O	652.3	996.1	960.2	975.5	975.3(01)	−55.4	−2.1
CO	730.1	1145.8	1052.3	1086.9	1086.7(05)	−12.9	−2.0
NH_3	841.2	1248.6	1230.7	1247.4	1247.9(04)	−89.0	−1.1
HCN	833.5	1363.5	1271.3	1311.0	1312.8(26)	−40.6	−1.4
CH_2O	1078.2	1611.5	1533.8	1568.0	1566.6(07)	−69.1	−2.7
CO_2	1033.4	1745.2	1573.6	1633.2	1632.5(05)	−30.3	−4.2
C_2H_2	1229.1	1742.5	1661.0	1697.1	1697.8(10)	−68.8	−1.9
CH_4	1374.1	1753.1	1747.0	1759.4	1759.3(06)	−115.9	−1.2
C_2H_4	1793.9	2379.3	2328.9	2360.8	2359.8(10)	−132.2	−2.1

[a] For vibrational and electronic corrections, see Ref. 1.

Table 8. Coupled-cluster atomization energies (kJ mol^{-1})

	CCSD(T)		CCSDT		CCSDTQ		Experiment	
	cc-pCV(56)Z		cc-pCV(Q5)Z		cc-pVTZ[a]		D_e	D_0
CH_2	757.9	−0.9	758.9	0.1	759.3	0.5	758.8	714.8 ± 1.8
H_2O	975.3	0.1	974.9	−0.3	975.7	0.5	975.2	917.8 ± 0.2
HF	593.2	0.0	593.0	−0.2	593.6	0.4	593.2	566.2 ± 0.7
N_2	954.7	−1.6	951.3	−5.0	955.2	−1.1	956.3	941.6 ± 0.2
F_2	161.0	−2.4	159.6	−3.8	162.9	−0.5	163.4	154.6 ± 0.6
CO	1086.7	0.0	1084.4	−2.3	1086.7	0.0	1086.7	1071.8 ± 0.5

[a] The CCSDTQ values have been obtained from the CCSDT/cc-pCV(Q5) results by adding quadruples corrections calculated in the cc-pVTZ basis.

is partly cancelled by the neglect of quadruples. Indeed, this situation is rather similar to that of the perturbative treatment of the connected doubles at the MP2 level of theory relative to the full CCSD treatment.

Reaction enthalpies

A property closely related to atomization energies are reaction enthalpies. In this section, we consider $\Delta_r H_e^\circ(0\,\mathrm{K})$, which represents the difference between the molecular equilibrium ground-state electronic energies of the products and of the reactants [Eqn (27)]:

$$\Delta_r H_e^\circ(0\ \mathrm{K}) = \sum_P E^P(\mathbf{R}_e) - \sum_R E^R(\mathbf{R}_e) \qquad (27)$$

We restrict ourselves to isogyric reactions, in which the number of paired electrons is conserved. For such reactions, we expect the coupled-cluster hierarchy to perform

Copyright © 2004 John Wiley & Sons, Ltd.

Table 9. Non-relativistic calculated and experimental electronic reaction enthalpies with calculated vibrational and relativistic corrections[a] (kJ mol^{-1}). The Hartree–Fock reaction enthalpies were calculated in the cc-pV6Z basis; the correlated reaction enthalpies were calculated with two-point extrapolation, at the all-electron cc-pcV(56)Z level. All calculations were carried out at the optimized all-electron CCSD(T)/cc-pCVQZ geometry

	Non-relativistic electronic reaction enthalpy						
Reaction	HF	MP2	CCSD	CCSD(T)	Exp.	Vib. corr.	Rel. corr.
$CO + H_2 \rightarrow CH_2O$	2.7	−25.0	−23.4	−23.0	−21.8(08)	30.2	0.7
$N_2 + 3H_2 \rightarrow 2NH_2$	−147.1	−164.4	−173.1	−165.5	−165.4(06)	86.1	1.6
$C_2H_2 + H_2 \rightarrow C_2H_4$	−214.1	−196.1	−209.7	−205.6	−203.9(12)	37.4	0.2
$CO_2 + 4H_2 \rightarrow CH_4 + 2H_2O$	−242.0	−237.3	−261.3	−244.7	−245.3(08)	92.7	1.0
$CH_2O + 2H_2 \rightarrow CH_4 + H_2O$	−246.5	−256.3	−257.2	−250.6	−251.9(09)	50.3	0.5
$CO + 3H_2 \rightarrow CH_4 + H_2O$	−243.8	−281.3	−280.5	−273.7	−273.8(08)	80.5	1.2
$HCN + 3H_2 \rightarrow CH_4 + NH_2$	−329.3	−316.0	−332.0	−321.5	−320.3(27)	85.4	0.9
$HNO + 2H_2 \rightarrow H_2O + NH_2$	−460.3	−466.0	−457.8	−446.3	−445.6(06)	56.7	1.0
$C_2H_2 + 3H_2 \rightarrow 2CH_4$	−466.6	−441.6	−458.6	−447.4	−446.7(13)	85.2	0.4
$CH_2 + H_2 \rightarrow CH_4$	−492.2	−571.6	−539.5	−543.4	−544.2(22)	46.8	0.4
$F_2 + H_2 \rightarrow 2HF$	−616.0	−601.4	−581.7	−567.3	−564.9(12)	17.6	1.6
$2CH_2 \rightarrow C_2H_4$	−731.8	−897.7	−830.1	−844.9	−845.7(31)	45.8	0.6
$O_3 + 3H_2 \rightarrow 3H_2O$	−1142.7	−939.7	−1010.1	−946.6	−935.5(17)	72.5	2.3

[a] For vibrational and electronic corrections, see Ref. 1.

better than for atomization energies,[8] where the number of paired electrons changes. Indeed, for the isogyric reactions in Table 9, the mean absolute errors in the calculated reaction enthalpies are 43.0, 13.5, 14.5 and 1.9 kJ mol^{-1},[8] respectively, for the Hartree–Fock, MP2, CCSD and CCSD(T) models, significantly smaller than the corresponding atomization-energy errors of 423.0, 36.2, 37.2 and 4.6 kJ mol^{-1}, respectively. The improvement in performance is particularly striking for the Hartree–Fock model, which for reaction enthalpies gives errors that are only three times larger than those obtained with the MP2 and CCSD models. Nevertheless, for chemical accuracy, we still need to take into account the effect of connected triples.

Also the basis-set convergence is faster for isogyric reaction enthalpies than for atomization energies.[8] From the mean absolute CCSD(T) errors in Tables 6 and 10, we note that whereas a quadruple-zeta basis with extrapolation is needed for convergence of the atomization energies to chemical accuracy, the reaction enthalpies are converged already in the triple-zeta basis without extrapolation. In Fig. 8, the normal distribution of errors in the calculated reaction enthalpies are plotted, illustrating the errors that arise at different levels of theory.

Table 10. Mean errors in the CCSD(T)/cc-pCV*X*Z reaction enthalpies (kJ mol^{-1}) relative to experiment. The extrapolated reaction enthalpies were obtained from the plain energies by using Eqn (25)

	DZ	TZ	QZ	5Z	6Z
plain	36.9	12.0	2.7	−0.3	−0.7
extr.		−2.0	−2.1	−1.7	−1.2

Hydrogen-bonding interaction energies

Having discussed the large energy changes associated with the breaking and making of covalent bonds, let us now consider briefly the much smaller changes that occur as a result of hydrogen bonding. Listed in Table 11 are the mean errors in the interaction energies of $(H_2O)_2$, $(HF)_2$, $(HCl)_2$, $HF \cdot H_2O$ and $HF \cdot HCN$, calculated at the MP2/aug-pV*XZ* levels of theory relative to MP2-R12 theory.[59] All calculations were carried out at the CCSD(T)/aug-cc-pVTZ optimized geometries of the dimers, using the experimental geometries for the monomers. For comparison, we note that the total MP2-R12 interaction energies are −7.0, −3.6, −13.5, −12.0 and −7.8 mE_h, respectively, for $(H_2O)_2$, $(HF)_2$, $(HCl)_2$, $HF \cdot H_2O$ and $HF \cdot HCN$.

A common problem with the calculation of interaction energies, in particular small interaction energies, is the basis-set superposition error.[1] Naively, we would calculate the interaction energy by subtracting the energies calculated for the monomers (separately, in the basis of each monomer) from the energy calculated for the dimer. However, in such a calculation, the dimer is represented in a larger basis than are the monomers, increasing the interaction energy beyond what would be obtained if all calculations had been carried out in the same basis. A better strategy is therefore to calculate the energy of each monomer in the full dimer basis, thereby ensuring a more uniform description of the constituent atoms in the dimer and in the separate monomers.[60,61] An interaction energy obtained in this manner is said to be counterpoise (CP) corrected. The CP correction to the interaction energy, that is the difference between the corrected and plain interaction energies, is always positive for variational wave functions (and in practice also for non-variational ones).

Copyright © 2004 John Wiley & Sons, Ltd.

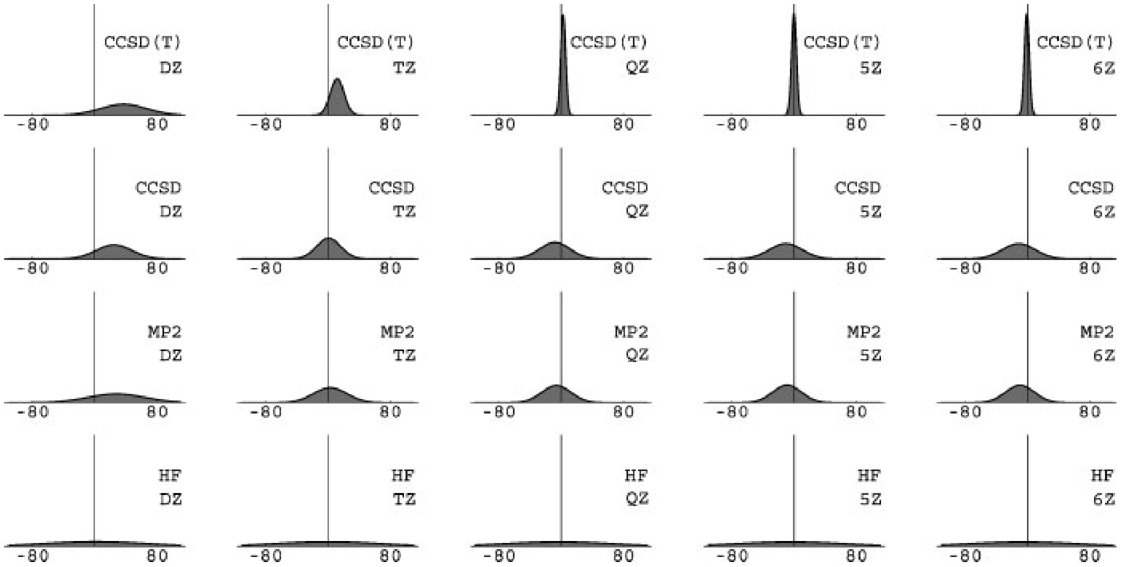

Figure 8. Normal distributions of errors in reaction enthalpies (kJ mol^{-1}), calculated with all electrons correlated

From Table 11, we see that the interaction energy converges from below without the CP correction applied but from above with this correction applied. Moreover, for small basis sets, the CP correction increases the error relative to the basis-set limit; for large basis sets, the CP correction reduces the error. More importantly, the CP correction makes the convergence smoother, as seen from the large improvement upon extrapolation of the CP corrected energies. By contrast, the uncorrected energies are hardly improved by extrapolation.

To understand this behavior, we recall that the two-point extrapolation formula Eqn (25) is designed to work only for basis-set errors that arise from a poor description of dynamic correlation. In the plain interaction energies, the error is dominated by the superposition error, which is not reduced by the extrapolation formula.[59] By contrast, in the CP corrected interaction energies, the basis-set superposition error has been removed and the remaining error arises from a poor description of dynamic correlation. Application of Eqn (25) removes most of this error, thereby accelerating convergence towards the basis-set limit.

Table 11. Mean errors in the hydrogen-bonding interaction energies of $(H_2O)_2$, $(HF)_2$, $(HCl)_2$, $HF \cdot H_2O$ and $HF \cdot HCN$ calculated at the MP2/aug-pV*X*Z levels of theory (μE_h), with and without the CP correction and with and without extrapolation using Eqn (25)

		DZ	TZ	QZ	5Z
No-CP	plain	−26	−247	−222	−160
	extr.		−340	−263	−95
CP	plain	988	420	188	104
	extr.		181	19	15

Two-electron Darwin term

In the previous sections, we have seen that atomization energies and reaction enthalpies both converge as X^{-3}. Not all molecular properties converge in the same manner with respect to the basis set, however. Consider, for example, the expectation value of the two-electron Darwin operator, Eqn (28):

$$V^{2D} = -\frac{1}{2}\alpha^2\pi\sum_{i\neq j}\delta(r_{ij}) \qquad (28)$$

which constitutes a part of the first-order relativistic correction to the electronic energy. From Fig. 3, we recall that the electronic wave function is particularly poorly represented at points of electron coalescence, suggesting a very slow convergence of the expectation value of this operator. Indeed, in the principal expansion, the error in the expectation value of the two-electron Darwin operator is inversely proportional to the cardinal number [Eqn (29)]:[62,63]

$$D_X^{2D} = D_\infty^{2D} + CX^{-1} \qquad (29)$$

In Table 12, we compare the convergence of the expectation value of the two-electron Darwin operator with and without the use of the two-point extrapolation formula Eqn (30),

$$D_\infty^{2D} = XD_X^{2D} - (X-1)D_{X-1}^{2D} \qquad (30)$$

obtained by elimination of C from Eqn (29).[62]

Without extrapolation, convergence to the basis-set limit is extremely slow, with errors as large as 28% in

Copyright © 2004 John Wiley & Sons, Ltd.

Table 12. Errors in the CCSD/cc-pV*X*Z expectation value of the two-electron Darwin operator Eqn (28) relative to the corresponding R12 values (μE_{h}). The extrapolated values were obtained by the two-point extrapolation formula Eqn (30)

		DZ	TZ	QZ	5Z	6Z	R12
He	plain	−7.1	−9.8	−11.0	−11.7	−12.1	−14.1
	extr.		−15.1	−14.7	−14.5	−14.3	
H_2	plain	−2.8	−3.5	−3.7	−3.9	−4.0	−4.4
	extr.		−4.9	−4.5	−4.5	−4.5	
HF	plain	−28.2	−38.1	−48.3	−53.7	−57.3	−74.8
	extr.		−57.9	−78.9	−75.5	−75.3	

the cc-pV6Z basis; with extrapolation, the errors are dramatically reduced to less than 5% in the cc-pVQZ basis. These calculations nicely illustrate, on the one hand, the very poor description of short-range interelectronic interactions by determinantal wave functions and, on the other, the very smooth convergence of these interactions afforded by the principal expansion.

Dipole moments

Many properties of molecular systems can conveniently be expressed in terms of derivatives of the electronic energy with respect to some external parameter. The dipole moment, for example, is obtained by differentiating the total energy with respect to the negative electric field strength. If we assume that Eqn (24) and therefore Eqn (25) is valid at all field strengths, we can differentiate Eqn (25) with respect to the field strength to yield the following formula for the dipole moment μ in the limit of an infinite basis [Eqn (31)]:[64]

$$\mu_\infty = \frac{X^3\mu_X - (X-1)^3\mu_{X-1}}{X^3 - (X-1)^3} \tag{31}$$

In Table 13, we used this formula to extrapolate to the basis-set limit of the dipole moments of BH and HF, calculated at the MP2, CCSD and CCSD(T) levels of theory, comparing with the corresponding R12 values.[64]

The calculations in Table 13 indicate that dipole moments converge in much the same manner as energies and that two-point extrapolation at the quadruple-zeta level reduces the error by about an order of magnitude. It is worth noting, however, that extrapolation works best when the basis set has been augmented with diffuse functions.[64] Without such functions added, the basis-set errors are not dominated by dynamic correlation and extrapolation is less effective. (In passing, we note that diffuse functions are also needed for the R12 method.) This situation is analogous to that of the interaction energies of hydrogen-bonded systems, for which extrapolation works well only when the calculated energies have been CP corrected.

Table 13. Mean MP2, CCSD and CCSD(T) errors (mea_0) relative to R12 theory for BH and HF. The extrapolated values were obtained using Eqn (31)

		DZ	TZ	QZ	5Z	6Z
cc-p(C)V*X*Z	plain	−14.7	−6.2	−2.3	−1.0	−0.8
	extr.		−2.7	0.6	0.4	−0.5
aug-cc-p(C)V*X*Z	plain	−15.8	−6.5	−2.7	−1.5	−0.9
	extr.		−2.7	0.1	−0.1	0.1

Bond distances

An important class of properties are the molecular spectroscopic constants, related to nuclear displacements. We begin the discussion of such properties by considering molecular equilibrium bond lengths in this subsection and continue with force constants in the next subsection.

The mean errors for the 27 bond distances in Table 14, calculated at the all-electron cc-pV*X*Z level of theory, are illustrated in Fig. 9. In general, molecular equilibrium bond lengths shorten with increasing cardinal number.[1,9] This behavior can be understood from the general observation that basis-set extension always favors the system with the lowest electronic energy. Since the pure electronic energy (which does not include the nuclear–nuclear repulsion energy) decreases as the internuclear

Table 14. Calculated and experimental bond distances (pm).[1,9] The calculations have been carried out in the cc-pCVQZ basis with all electrons correlated

Molecule	Bond distance	HF	MP2	CCSD	CCSD(T)	Exp.
H_2	R_{HH}	73.4	73.6	74.2	74.2	74.1
HF	R_{FH}	89.7	91.7	91.3	91.6	91.7
H_2O	R_{OH}	94.0	95.7	95.4	95.7	95.7
HOF	R_{OH}	94.5	96.6	96.2	96.6	96.6
H_2O_2	R_{OH}	94.1	96.2	95.8	96.2	96.7
HNC	R_{NH}	98.2	99.5	99.3	99.5	99.4
NH_3	R_{NH}	99.8	100.8	100.9	101.1	101.1
N_2H_2	R_{NH}	101.1	102.6	102.5	102.8	102.9
C_2H_2	R_{CH}	105.4	106.0	106.0	106.2	106.2
HCN	R_{CH}	105.7	106.3	106.3	106.6	106.5
C_2H_4	R_{CH}	107.4	107.8	107.9	108.1	108.1
CH_4	R_{CH}	108.2	108.3	108.5	108.6	108.6
N_2	R_{NN}	106.6	110.8	109.1	109.8	109.8
CH_2O	R_{CH}	109.3	109.8	109.9	110.1	110.1
CH_2	R_{CH}	109.5	110.1	110.5	110.7	110.7
CO	R_{CO}	110.2	113.2	112.2	112.9	112.8
HCN	R_{CN}	112.3	116.0	114.6	115.4	115.3
CO_2	R_{CO}	113.4	116.4	115.3	116.0	116.0
HNC	R_{CN}	114.4	117.0	116.2	116.9	116.9
C_2H_2	R_{CC}	117.9	120.5	119.7	120.4	120.3
CH_2O	R_{CO}	117.6	120.6	119.7	120.4	120.3
N_2H_2	R_{NN}	120.8	124.9	123.6	124.7	124.7
O_3	R_{OO}	119.2	127.6	124.1	126.6	127.2
C_2H_4	R_{CC}	131.3	132.6	132.5	133.1	133.1
F_2	R_{FF}	132.7	139.5	138.8	141.1	141.2
HOF	R_{OF}	136.2	142.0	141.2	143.3	143.4
H_2O_2	R_{OO}	138.4	144.3	143.1	145.0	145.6

Copyright © 2004 John Wiley & Sons, Ltd.

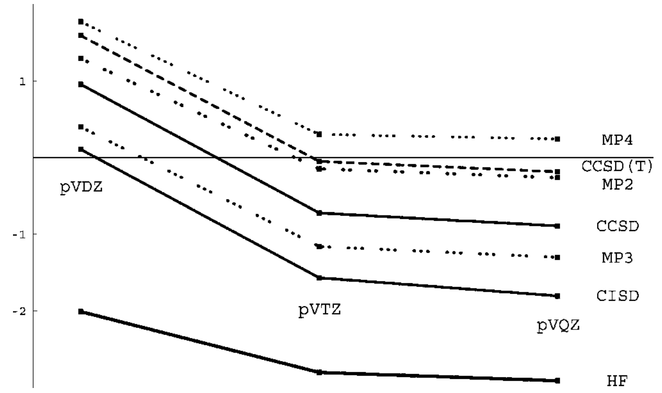

Figure 9. Mean errors relative to experiment in calculated bond distances (pm). The bond distances have been calculated in the cc-pV*XZ* basis sets with all electrons correlated

Table 15. Mean absolute errors relative to experiment in calculated bond distances (pm)

$\lvert\bar{\Delta}\rvert$	cc-pVDZ	cc-pVTZ	cc-pVQZ
HF	1.94	2.63	2.74
MP2	1.35	0.56	0.51
CCSD	1.19	0.64	0.80
CCSD(T)	1.68	0.20	0.16

separation tends to zero, we conclude that bonds become shorter with increasing cardinal number.

As expected, the bond-length shortening upon basis-set extension is less pronounced for the Hartree–Fock model (e.g. 0.8 pm from cc-pVDZ to cc-pVTZ) than for the correlated models (1.6 pm for the same extension).[1,65] This difference between the Hartree–Fock and correlated models can be understood from the fact that, in the Hartree–Fock model, the added orbitals only contribute to charge polarization; in the correlated models, they also improve the virtual excitation space.

From Fig. 9, we also note that bonds lengthen with improvements in the *N*-electron model, being shortest at the Hartree–Fock level. This behavior, which can be understood from the fact that the correlated electrons occupy antibonding as well as bonding orbitals, creates a considerable scope for cancellation of basis-set and *N*-electron errors. In the small cc-pVDZ basis, for example, the simple CISD model and the third-order Møller–Plesset (MP3) model have the smallest mean errors of all methods, while the most elaborate models such as the CCSD(T) and fourth-order Møller–Plesset (MP4) models have the largest errors. However, as we increase the basis set, the situation reverses as the CCSD(T) and MP4 models improve their performance while the CISD and MP3 models do not. Figure 9 also illustrates the typical oscillations of the Møller–Plesset series: bond lengths shorten from MP2 to MP3 but lengthen from MP3 to MP4.[1]

As seen from Fig. 9, the more accurate models should always be used with basis sets of at least triple-zeta quality, see also Table 15, where the mean absolute errors in the bond distances of the Hartree–Fock, MP2, CCSD and CCSD(T) models are listed. In the cc-pVDZ basis, the CCSD(T) error is almost as large as the Hartree–Fock error; by contrast, in the cc-pVQZ basis, the CCSD(T) error is more than an order of magnitude smaller than the Hartree–Fock error.

In Table 14, we listed the calculated and experimental bond distances for a few selected systems. We note in particular the high accuracy of the CCSD(T) model,[1,9,65] with mean errors of 1.68, 0.01 and -0.12 pm in the cc-pVDZ, cc-pVTZ and cc-pVQZ basis sets, respectively; the corresponding mean absolute errors are 1.68, 0.20 and 0.16 pm. However, even this high accuracy arises in part from error cancellation, the bond distances are further shortened by about 0.1 pm upon basis-set extension from cc-pVQZ to cc-pV6Z[46,66–68] and by 0.02 pm upon triples relaxation from CCSD(T) to CCSDT.[69,70] We conclude that the intrinsic error of the CCSDT model is about -0.2 pm. Indeed, calculations with the CCSDTQ model confirm that the introduction of connected quadruples increases bond lengths by 0.1 to 0.2 pm.

Spectroscopic constants

The frequency of a diatomic fundamental transition is given by $\nu = \omega_e - 2\omega_e x_e$, where the harmonic constant ω_e can be calculated from second derivatives of the potential-energy surface, whereas the calculation of the anharmonic constant $\omega_e x_e$ also requires third and fourth derivatives (see for instance Ref. 71). In the present section, we consider the accuracy of the calculated spectroscopic constants of the diatomics BH, HF, CO, N_2 and F_2; for comparison, we include their bond lengths in this discussion.

In Figs. 10–12, normal distributions of errors in the equilibrium bond lengths, harmonic constants and anharmonic constants, respectively, are plotted for the five diatomics.[67] These figures also contain the mean absolute errors, printed next to the normal distribution plots. All calculations have been carried out in the core–valence cc-pCV*XZ* basis sets, with all electrons correlated and at the optimized geometry of the given computational model.

Although the performance of the different models is similar for the three spectroscopic constants, some differences are apparent. In general, there is a significant improvement in the performance in the sequence Hartree–Fock, CCSD and CCSD(T). The uncorrelated Hartree–Fock model performs particularly poorly for the harmonic constants, with mean absolute errors of almost 300 cm^{-1}, that is, 30 times larger than the errors of the CCSD(T) model; for the anharmonic constants, by contrast, the Hartree–Fock performance is fairly decent, with mean absolute errors of only 4 cm^{-1}.

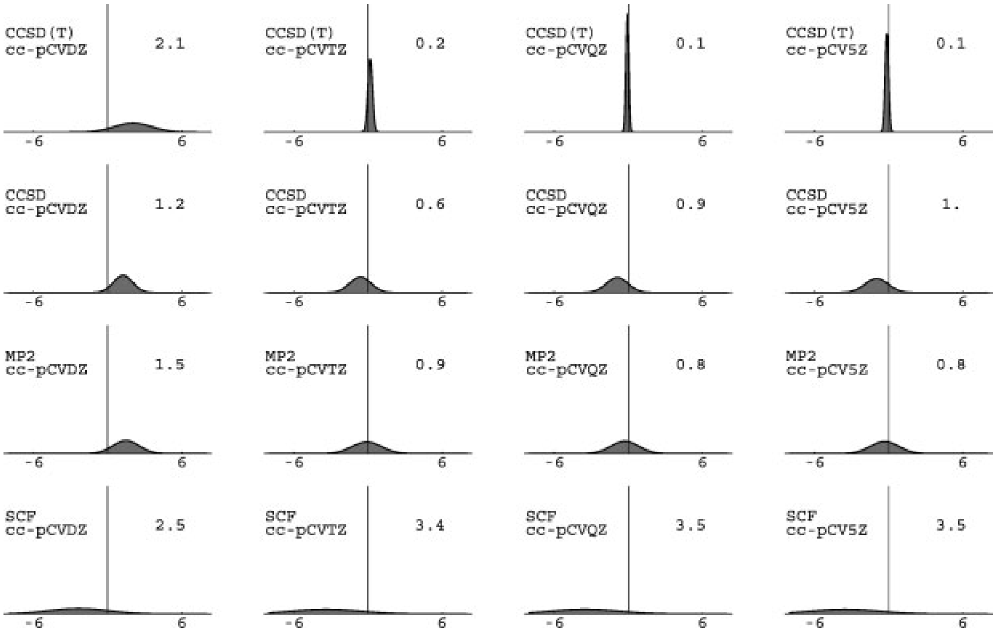

Figure 10. Normal distributions of the errors in the bond distances of BH, HF, CO, N_2 and F_2 relative to experiment, calculated in the cc-pCV*X*Z basis sets with all electrons correlated (pm). Next to each normal-distribution plot, the corresponding mean absolute error has been printed

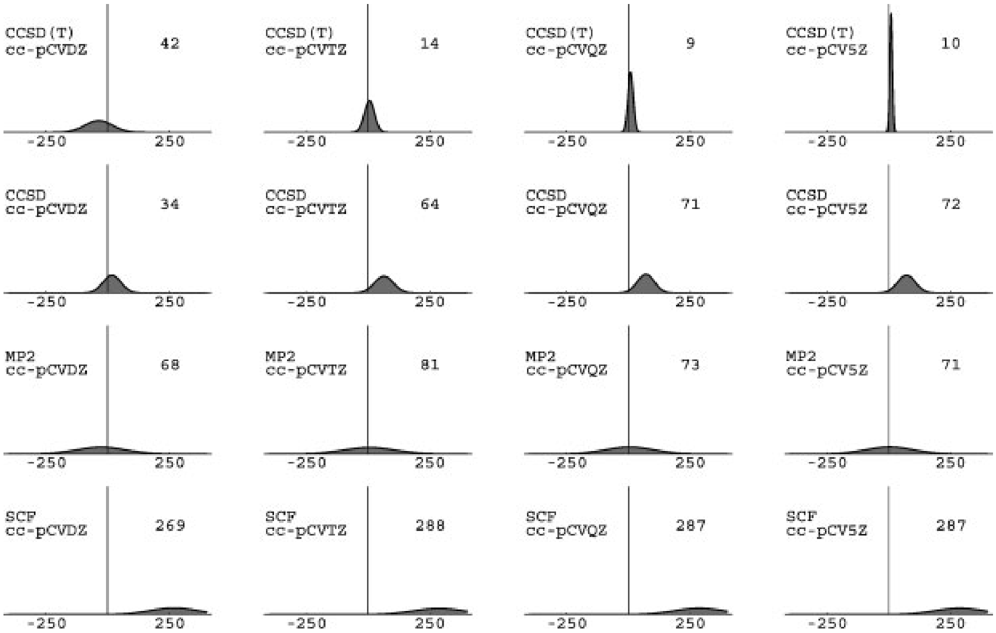

Figure 11. Normal distributions of the errors in the harmonic constants ω_e of BH, HF, CO, N_2 and F_2 relative to experiment, calculated in the cc-pCV*X*Z basis sets with all electrons correlated (cm^{-1}). Next to each normal-distribution plot, the corresponding mean absolute error has been printed

The CCSD description is for all spectroscopic constants a definite improvement on the Hartree–Fock description, with an error reduction of about a factor of four (in the largest basis). For the anharmonic constants, we note a rather sharp but off-center normal distribution in the triple-zeta basis, indicating a very systematic underestimation by about $2\,cm^{-1}$. However, since our statistics are based on only five constants, it could be that this behavior is not typical of the CCSD model.

Next, introducing connected triple excitations at the CCSD(T) level, we note a further significant reduction in errors, by about an order of magnitude relative to the CCSD model. It is worth noting that this improvement is

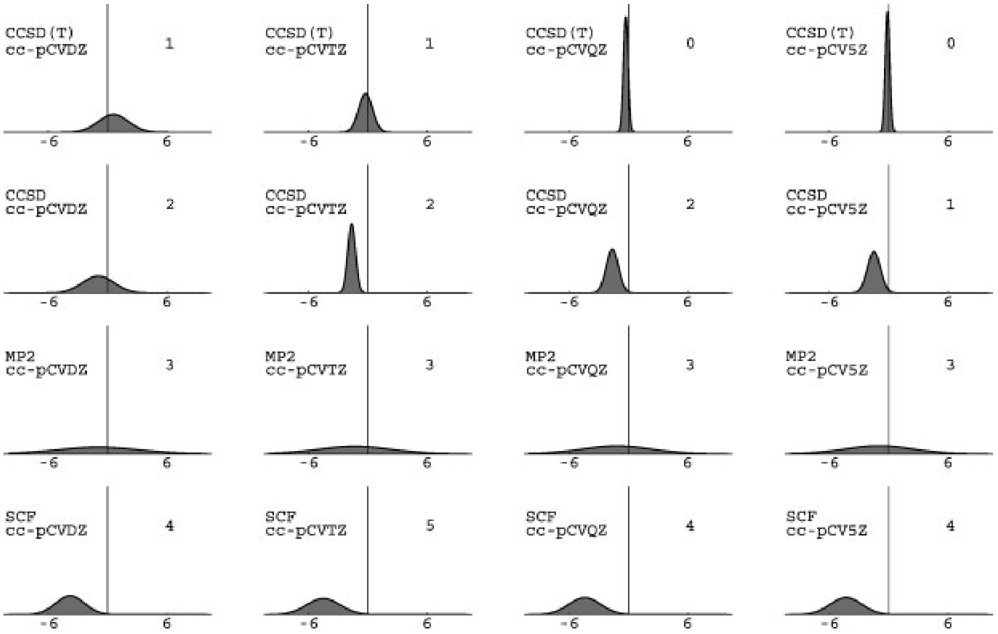

Figure 12. Normal distributions of the errors in the anharmonic constants $\omega_e x_e$ of BH, HF, CO, N_2 and F_2 relative to experiment, calculated in the cc-pCV*X*Z basis sets with all electrons correlated (cm^{-1}). Next to each normal-distribution plot, the corresponding mean absolute error has been printed

observed only in the cc-pCVQZ and cc-pCV5Z basis sets. While some improvement on the CCSD model is also observed in the cc-pCVTZ basis, the cc-pCVDZ basis is too small for use with the CCSD(T) model.

The MP2 model differs from the CCSD model only in that the doubles amplitudes have been determined by perturbation theory rather than from the coupled-cluster equations. However, this difference has an enormous impact on the harmonic and anharmonic constants, leading to much broader distributions of errors than those of the CCSD model. By contrast, for bond distances (and indeed for the other properties discussed in this paper), the MP2 model performs as well as the CCSD model. Apparently, the MP2 scheme is less well suited than the more expensive CCSD model to the calculation of properties related to bond stretching and more generally to bond-breaking processes.

The plots in Figs. 10–12 also nicely illustrate the general observation that a perturbative treatment of the cluster amplitudes usually leads to an overestimation of the amplitudes. Thus, the MP2 normal distributions are not just broader than the corresponding CCSD distributions but are also displaced relative to these distributions, always away from the Hartree–Fock distributions.

Concerning the direction of change in the calculated spectroscopic constants, we first note that the harmonic and anharmonic constants decrease with improvements in the *N*-electron treatment, as we would expect from the fact that such improvements are particularly important at large distances, lowering this part of the potential-energy curve relative to the inner part. For the same reason, the equilibrium bond distances lengthen with improvements in the *N*-electron treatment.

With respect to basis-set improvements, the situation is more complicated because of two competing effects. At a fixed geometry (e.g. the experimental equilibrium geometry), the harmonic and anharmonic force constants are always reduced by basis-set improvements since, upon basis-set extension, the inner part of the potential-energy curve is lowered more than the outer part, thereby reducing all even-order geometry derivatives. If instead these force constants are evaluated at the optimized geometry (which changes with the basis set), then there is a competing effect from the purely nuclear contributions to the constants. Since basis-set extension leads to bond contraction and thus to larger nuclear derivative contributions, it increases the calculated force constants. In most cases, these purely nuclear contributions dominate, resulting in an overall increase in the calculated force constant upon basis-set extension. Exceptions are common for small basis sets at the Hartree–Fock level.

From the above discussion, we have seen that the intrinsic error in the CCSD(T) harmonic constants are fairly large (about $10\,\text{cm}^{-1}$),[67] making the accurate calculation of fundamental vibrational transitions to within say $1\,\text{cm}^{-1}$ a very difficult business indeed. In the following, we will use the N_2 molecule to illustrate how such an accuracy can nevertheless be achieved. Before we begin, we recall that the anharmonic contribution to the fundamentals constitutes much less of a problem (at least for semi-rigid molecules), since

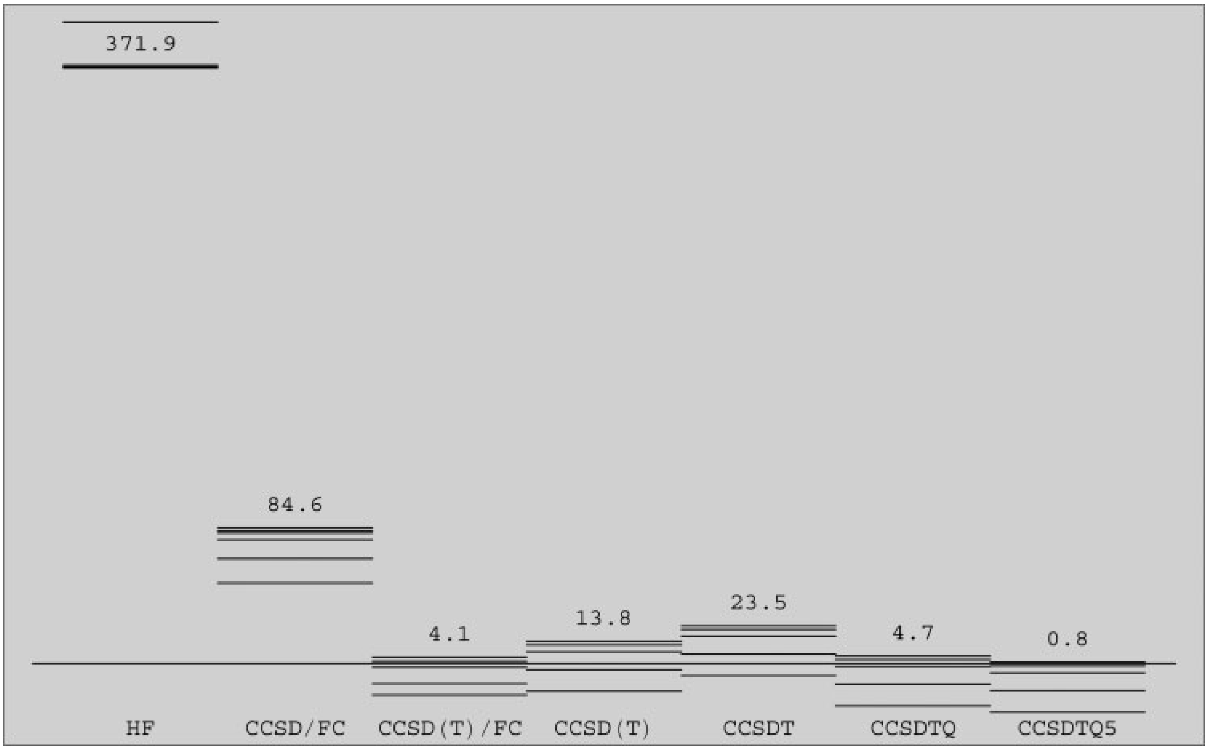

Figure 13. Errors in the calculated harmonic vibrational constant ω_e of N_2 relative to experiment (cm^{-1}), calculated at different levels of coupled-cluster theory. At each level of theory, the horizontal lines represent calculations in different basis sets

convergence to within 1 cm^{-1} is achieved already at the CCSD(T)/cc-pCVTZ level of theory. In our discussion, we therefore consider only the difficult harmonic contribution to the vibrational transitions.

In Fig. 13, we have illustrated the different contributions to the harmonic vibrational frequency of N_2. At the Hartree–Fock level of theory, the error is 371.9 cm^{-1} in the basis-set limit.[67] Unlike at the correlated levels of theory, the harmonic frequency decreases as we go from cc-pVDZ to cc-pVTZ (by almost 30 cm^{-1}) and also from cc-pVTZ to cc-pVQZ (by 2 cm^{-1}), after which it increases by less than 1 cm^{-1} as the basis set is further extended.

Next in Fig. 13, we carried out a series of CCSD/cc-pV*XZ* calculations, with only the valence electrons correlated.[67] The calculated harmonic frequency now increases rather than decreases with increasing cardinal number; moreover, the basis-set differences are larger than at the uncorrelated Hartree–Fock level. In the basis-set limit, we are still off by as much as 85 cm^{-1} from the experimental harmonic frequency, which is typical of descriptions based on the use of connected doubles only.

Introducing connected triples at the valence-electron CCSD(T)/cc-pV*XZ* level of theory, we arrive at a rather small error of 4 cm^{-1} in the basis-set limit; see Fig. 13.[67] The good agreement with experiment is fortuitous, however, and occurs as a result of a near cancellation of the errors arising from the neglect of core correlation, from the approximate (perturbative) treatment of the triples and from the neglect of quadruple and higher-order connected excitations.[67,68] Indeed, as we introduce core correlation at the all-electron CCSD(T)/cc-pCV*XZ* level of theory, the error increases by almost 10 cm^{-1}. A similar large increase in the error occurs as we replace the perturbative triples by fully relaxed triples at the all-electron CCSDT level of theory.

The surprisingly large CCSDT error of 24 cm^{-1} in Fig. 13 indicates that quadruples and higher connected excitations are important for the accurate calculation of harmonic frequencies. Indeed, at the CCSDTQ level of theory, the error in the N_2 harmonic frequency is reduced to 5 cm^{-1}.[72,73] Finally, at the CCSDTQ5 level of theory, we are within 1 cm^{-1} of the exact non-relativistic limit. Adding a relativistic correction of -1.4 cm^{-1},[75] we finally obtain a frequency of 2358.0 cm^{-1}, just below the experimental harmonic frequency of 2358.6 cm^{-1}.

Coupled-cluster excitation-level convergence

Having examined the coupled-cluster convergence of a variety of molecular properties in the previous subsections, let us now summarize by comparing the convergence for some of these properties. In Plate 3, we have plotted, on a logarithmic scale, the errors in the calculated harmonic force constants, equilibrium bond distances and atomization energies as functions of the

Copyright © 2004 John Wiley & Sons, Ltd.

highest included virtual excitation level in coupled-cluster theory. The errors relative to experiment are reduced by several factors with each new level, the CCSDT errors being an order of magnitude smaller than the Hartree–Fock errors. The CCSD(T) errors have not been included in these plots but are usually smaller than the CCSDT errors because of cancellation of the errors arising from an approximate treatment of the triples and the neglect of quadruples.

The coupled-cluster hierarchy clearly provides us with a well-defined path towards the exact solution of the Schrödinger equation, at least for single-configurational systems dominated by the Hartree–Fock configuration. Indeed, at the CCSDTQ or CCSDTQ5 levels of theory, we have exhausted the Schrödinger equation in the sense that relativistic corrections henceforth become as important as further correlation corrections, see Plate 3. We note, however, that for systems containing heavier atoms, this cross-over could occur at a lower level of coupled-cluster theory. Indeed, for very heavy atoms, the relativistic corrections are sometimes more important than those of electron correlation.[74–77]

CONCLUSIONS

We have reviewed the accurate calculation of molecular properties by coupled-cluster theory. In particular, we have demonstrated that, for a rigorous calculation of such properties to some prescribed accuracy, it is necessary to carry out sequences of electronic-structure calculations where we systematically explore the flexibility in the one- and N-electron descriptions of the electronic system, carefully monitoring the convergence in the calculated properties. In the N-electron hierarchy, we improve the description by including higher and higher virtual excitations in the wave function, providing an increasingly more detailed description of the virtual electronic processes. In the one-electron hierarchy, our description of the electronic system is improved by extending the virtual excitation space, as required for an accurate representation of the included virtual excitations. In particular, we have discussed the calculation of molecular properties at the Hartree–Fock, CCS, CCSD, CCSDT, CCSDTQ and CCSDTQ5 levels of theory, including up to quintuple connected virtual excitations in the calculations. To expand the virtual excitation spaces in an optimal manner, we have made use of the correlation-consistent valence and core–valence cc-p(C)VXZ one-electron basis sets, with cardinal numbers $2 \leq X \leq 6$.

We have demonstrated that, in correlation-consistent coupled-cluster theory, calculated molecular properties converge in a predictable manner. In particular, as we increase the virtual excitation level, errors are reduced linearly, typically by a factor of three or four at each new level. In this way, convergence to chemical accuracy is sometimes achieved with the inclusion of triple excitations but more often quadruple or even quintuple excitations are needed. In the one-electron correlation-consistent hierarchy, convergence is much slower, with an error in many properties proportional to X^{-3}. However, because of the very smooth convergence with the cardinal number, it is often possible to extrapolate the results obtained with finite cardinal numbers to the limit of an infinite basis set, making it possible to estimate the basis-set limit at each level of coupled-cluster theory.

Because of the very high cost of coupled-cluster theory, the highest included virtual excitation level is sometimes determined in an approximate manner, using perturbation theory. Particularly important are the MP2 and CCSD(T) models, which can be taken as approximations to the CCSD and CCSDT models where the doubles and triples, respectively, are determined by perturbation theory rather than by coupled-cluster theory. These approximations are very useful, reducing the computational cost significantly at little loss of accuracy. Indeed, because of systematic error cancellation, the CCSD(T) model is for many properties such as atomization energies, equilibrium bond distances and force constants more accurate (but less flexible and robust) than the more expensive CCSDT model, in part explaining the great success of CCSD(T) theory in high-accuracy computational quantum chemistry.

Because of the separate expansions of the one- and N-electron hierarchies in coupled-cluster theory, cancellations frequently occur between the errors arising from the one- and N-electron truncations, leading to a fortuitously good agreement with experiment. We emphasize, however, that agreement with experiment for a few selected properties is not in itself a guarantee of quality and should never be taken as indicative of an accurate description of the electronic system. To ensure such a description, the errors arising from the one- and N-electron truncations must be controlled by carrying out sequences of calculations, where the different levels of theory are systematically varied and where convergence is carefully monitored. Only when carried out in this manner does coupled-cluster theory constitute a truly predictive tool in quantum chemistry.

Acknowledgments

This work was supported by the Norwegian Research Council through a Strategic University Program in Quantum Chemistry (Grant No 154011/420) and through a grant of computer time from the Supercomputing Programme (T.H. and T.R.). P.J. and J.O. acknowledge support from the Danish Natural Research Council (Grant 21-02-0467) and from the Danish Center for Scientific Computing (DCSC). The research of W.K. was supported by the Deutsche Forschungsgemeinschaft through the Center for Functional Nanostructures (CFN, Project No. C2.3).

Copyright © 2004 John Wiley & Sons, Ltd.

REFERENCES

1. Helgaker T, Jørgensen P, Olsen J. *Molecular Electronic-Structure Theory.* Wiley: Chichester, 2000.
2. Jensen F. *Introduction to Computational Chemistry.* Wiley: Chichester, 1999.
3. Cioslowski J (ed). *Quantum-Mechanical Prediction of Thermochemical Data.* Kluwer Academic Publishers: Dordrecht, 2001.
4. Dunning TH Jr. *J. Phys. Chem. A* 2000; **104**: 9062–9080.
5. Ayers PW, Yang W. In *Computational Medicinal Chemistry for Drug Discovery*, Bultnick P, De Winter H, Langenaeker W, Tollenaere JP (eds). Marcel Dekker Inc: Basel, 2004; 89–118.
6. Császár, AG, Allen WD, Schaefer HF III. *J. Chem. Phys.* 1998; **108**: 9751–9764.
7. Dunning TH Jr, Peterson KA, Woon DE. In *Encyclopedia of Computational Chemistry*, vol. 1, Schleyer PV, Allinger NL, Clark T, Gasteiger J, Kollman PA, Schaefer HF III, Scheiner PR (eds). J. Wiley & Sons: New York, 1998; 88–115.
8. Bak KL, Jørgensen P, Olsen J, Helgaker T, Klopper W. *J. Chem. Phys.* 2000; **112**: 9229–9242.
9. Bak KL, Gauss J, Jørgensen P, Olsen J, Helgaker T, Stanton JF. *J. Chem. Phys.* 2001; **114**: 6548–6556.
10. Bartlett RJ. In *Modern Electronic Structure Theory*, Yarkony DR (ed). World Scientific: Singapore, 1995; 1047–1131.
11. Helgaker T, Jørgensen P, Olsen J, Klopper W. In *Computational Medicinal Chemistry for Drug Discovery*, Bultnick P, De Winter H, Langenaeker W, Tollenaere JP (eds). Marcel Dekker: Basel, 2004; 57–88.
12. Saebø S, Pulay P. *J. Chem. Phys.* 2001; **115**: 3975–3983.
13. Ayala PY, Scuseria GE. *J. Chem. Phys.* 1999; **110**: 3660–3671.
14. Ayala PY, Scuseria GE. *J. Chem. Phys.* 1999; **111**: 8330–8343.
15. Schütz M, Hetzer G, Werner H-J. *J. Chem. Phys.* 1999; **111**: 5691–5705.
16. Schütz M, Werner H-J. *J. Chem. Phys.* 2001; **114**: 661–681.
17. Schütz M. *J. Chem. Phys.* 2002; **116**: 8772–8785.
18. Lee MS, Maslen PE, Head-Gordon M. *J. Chem. Phys.* 2000; **112**: 3592–3601.
19. Atkins PW, Friedman RS. *Molecular Quantum Mechanics* (3rd edn). Oxford University Press: New York, 1997.
20. Tuma C, Boese AD, Handy NC. *Phys. Chem. Chem. Phys.* 1999; **1**: 3939–3948.
21. Almöf J. In *Modern Electronic Structure Theory: Part I*, Yarkony DR (ed). World Scientific: New York, 1995; 110–151.
22. Pulay P. In *Modern Electronic Structure Theory*, Yarkony DR (ed). World Scientific: New York, 1995; 1191–1240.
23. Barszczewicz A, Helgaker T, Jaszuński M, Jørgensen P, Ruud K. *J. Chem. Phys.* 1994; **101**: 6822–6828.
24. Purvis GD, Bartlett RJ. *J. Chem. Phys.* 1982; **76**: 1910–1918.
25. Siegbahn PEM. In *Lecture Notes in Quantum Chemistry*, Roos BO (ed). Springer: Berlin, Heidelberg, 1992; 255–294.
26. Christiansen O, Halkier A, Koch H, Jørgensen P, Helgaker T. *J. Chem. Phys.* 1998; **108**: 2801–2816.
27. Noga J, Bartlett RJ. *J. Chem. Phys.* 1987; **86**: 7041–7050.
28. Scuseria GE, Schaefer HF III. *Chem. Phys. Lett.* 1988; **152**: 382–386.
29. Ruden TA, Helgaker T, Olsen J, Jørgensen P. *Chem. Phys. Lett.* 2003; **371**: 62–67.
30. Kucharski SA, Bartlett RJ. *J. Chem. Phys.* 1992; **97**: 4282–4288.
31. Olsen J. *J. Chem. Phys.* 2000; **113**: 7140–7148.
32. Olsen J, Christiansen O, Koch H, Jørgensen P. *J. Chem. Phys.* 1996; **105**: 5082–5090.
33. Christiansen O, Olsen J, Jørgensen P, Koch H, Malmqvist PÅ. *Chem. Phys. Lett.* 1996; **261**: 369–378.
34. Raghavachari K, Trucks GW, Head-Gordon M, Pople JA. *Chem. Phys. Lett.* 1989; **157**: 479–483.
35. Bak KL, Jørgensen P, Olsen J, Helgaker T, Gauss J. *Chem. Phys. Lett.* 2000; **317**: 116–122.
36. Boys S. *Proc. Roy. Soc. A* 1950; **200**: 542–554.
37. Helgaker T, Taylor PR. In *Modern Electronic Structure Theory: Part II*, Yarkony DR (ed). World Scientific: New York, 1995; 725–856.
38. Feller D, Davidson ER. In *Review in Computational Chemistry*, Lipkowitz KP, Boyd DB (eds). VCH Publishers: New York, 1990; 1–37.
39. Carroll DP, Silverstone HJ, Metzger RM. *J. Chem. Phys.* 1979; **71**: 4142–4163.
40. Bunge CF. *Theor. Chim. Acta* 1970; **15**: 126.
41. Klopper W, Schütz M, Lüthi HP, Leutwyler S. *J. Chem. Phys.* 1995; **103**: 1085–1098.
42. Hylleraas EA. *Adv. Quantum Chem.* 1964; **1**: 1–33.
43. Noga J, Kutzelnigg W, Klopper W. *Chem. Phys. Lett.* 1992; **199**: 497–504.
44. Klopper W, Kutzelnigg W. *Chem. Phys. Lett.* 1987; **134**: 17–22.
45. Dunning TH Jr. *J. Chem. Phys.* 1989; **90**: 1007–1023.
46. Wilson AK, van Mourik T, Dunning TH Jr. *J. Mol. Struct. (THEOCHEM)* 1996; **388**: 339–349.
47. Woon DE, Dunning TH Jr. *J. Chem. Phys.* 1993; **98**: 1358–1371.
48. Koput J, Peterson KA. *J. Phys. Chem. A* 2002; **106**: 9595–9599.
49. Woon DE, Dunning TH Jr. *J. Chem. Phys.* 1995; **103**: 4572–4585.
50. Peterson KA, Dunning TH Jr. *J. Chem. Phys.* 2002; **117**: 10548–10560.
51. Kendall RA, Dunning Jr TH, Harrison RJ. *J. Chem. Phys.* 1992; **96**: 6796–6806.
52. Helgaker T, Klopper W, Koch H, Noga J. *J. Chem. Phys.* 1997; **106**: 9639–9646.
53. Halkier A, Helgaker T, Jørgensen P, Klopper W, Koch H, Olsen J, Wilson AK. *Chem. Phys. Lett.* 1998; **286**: 243–252.
54. Helgaker T, Klopper W, Halkier H, Bak KL, Jørgensen P, Olsen J. In *Highly Accurate* Ab Initio *Computation of Thermochemical Data*, Cioslowski J (ed). Kluwer: Dordrecht, 2001; 1–30.
55. Martin JML, de Oliveira G. *J. Chem. Phys.* 1999; **111**: 1843–1856.
56. Boese AD, Oren M, Atasoylu O, Martin JML, Kállay M, Gauss J. *J. Chem. Phys.* 2004; **120**: 4129–4141.
57. Frisch MJ, Trucks GW, Schlegel HB, Scuseria GE, Robb MA, Cheeseman JR, Montgomery JA Jr, Vreven T, Kudin KN, Burant JC, Millam JM, Iyengar SS, Tomasi J, Barone V, Mennucci B, Cossi M, Scalmani G, Rega N, Petersson GA, Nakatsuji H, Hada M, Ehara M, Toyota K, Fukuda R, Hasegawa J, Ishida M, Nakajima T, Honda Y, Kitao O, Nakai H, Klene M, Li X, Knox JE, Hratchian HP, Cross JB, Adamo C, Jaramillo J, Gomperts R, Stratmann RE, Yazyev O, Austin AJ, Cammi R, Pomelli C, Ochterski JW, Ayala PY, Morokuma K, Voth GA, Salvador P, Dannenberg JJ, Zakrzewski VG, Dapprich S, Daniels AD, Strain MC, Farkas O, Malick DK, Rabuck AD, Raghavachari K, Foresman JB, Ortiz JV, Cui Q, Baboul AG, Clifford S, Cioslowski J, Stefanov BB, Liu G, Liashenko A, Piskorz P, Komaromi I, Martin RL, Fox DJ, Keith T, Al-Laham MA, Peng CY, Nanayakkara A, Challacombe M, Gill PMW, Johnson B, Chen W, Wong MW, Gonzalez C, Pople JA. *Gaussian 03, Revision A.1*. Gaussian: Pittsburgh PA, 2003.
58. Klopper W, Noga J. *Chem. Phys. Chem.* 2003; **4**: 32–48.
59. Halkier A, Klopper W, Helgaker T, Jørgensen P, Taylor PR. *J. Chem. Phys.* 1999; **111**: 9157–9167.
60. Boys SF, Bernardi B. *Mol. Phys.* 1970; **19**: 553.
61. van Duijneveldt FB, van Duijneveldt-van de Rijdt JGCM, van Lenthe JH. *Chem. Rev.* 1994; **94**: 1873–1885.
62. Halkier A, Helgaker T, Klopper W, Olsen J. *Chem. Phys. Lett.* 2000; **319**: 287–295.
63. Salomonsen S, Öster P. *Phys. Rev. A* 1989; **40**: 5548–5558.
64. Halkier A, Klopper W, Helgaker T, Jørgensen P. *J. Chem. Phys.* 1999; **111**: 4424–4430.
65. Helgaker T, Gauss J, Jørgensen P, Olsen J. *J. Chem. Phys.* 1997; **106**: 6430–6440.
66. Peterson KA, Wilson AK, Woon DE, Dunning TH Jr. *Theor. Chim. Acta* 1997; **97**: 251–259.
67. Pawlowski F, Halkier A, Jørgensen P, Bak KL, Helgaker T, Klopper W. *J. Chem. Phys.* 2003; **118**: 2539–2549.
68. Martin JML. *Chem. Phys. Lett.* 1998; **292**: 411–420.
69. Halkier A, Jørgensen P, Gaüss J, Helgaker T. *J. Chem. Phys. Lett.* 1997; **274**: 235–241.
70. Feller DA, Sordo JA. *J. Chem. Phys.* 2000; **112**: 5604–5610.
71. Papousek D, Aliev MR. *Molecular Vibrational-Rotational Spectra.* Academia: Prague, 1982.
72. Kucharski SA, Watts JD, Bartlett R. *J. Chem. Phys. Lett.* 1999; **302**: 295–301.
73. Krogh JW, Olsen J. *Chem. Phys. Lett.* 2001; **344**: 578–586.
74. Visscher L, Dyall KG. *J. Chem. Phys.* 1996; **104**: 9040–9045.
75. Visscher L, Styszyñski J, Nieuwpoort W. *J. Chem. Phys.* 1996; **105**: 1987–1994.
76. de Jong WA, Styszyñski J, Visscher L, Nieuwpoort W. *J. Chem. Phys.* 1998; **108**: 5177–5184.
77. Fossgaard O, Gropen O, Corral Valero M, Saue T. *J. Chem. Phys.* 2003, **118**: 10418–10430.

Copyright © 2004 John Wiley & Sons, Ltd.